

Aus der Klinik für Pädiatrie mit Schwerpunkt Neurologie
und dem Institut für Zell- und Neurobiologie
der Medizinischen Fakultät Charité – Universitätsmedizin Berlin

DISSERTATION

Cyclin-dependent kinase 5 regulatory subunit-associated protein 2 (Cdk5rap2) in neuronal differentiation and germ cell pool maintenance

zur Erlangung des akademischen Grades
Medical Doctor - Doctor of Philosophy (MD/PhD)
im Rahmen des
International Graduate Program Medical Neurosciences

vorgelegt der Medizinischen Fakultät
Charité – Universitätsmedizin Berlin

von

Sami Zaqout

aus: Gaza, Palästina

Datum der Promotion: 22. September 2017

*“Knowledge exists potentially in the human soul like the seed in the soil;
by learning the potential becomes actual.”*

Muhammad Al-Ghazali

To my mother

To my wife

and

To my lovely children: Ismail, Ali and Sama

Table of contents

Table of contents	i
Figures	iii
Abstract	iv
Zusammenfassung	vi
1. Introduction	1
1.1 Autosomal recessive primary microcephaly (MCPH)	1
1.2 MCPH pathomechanisms	1
1.3 MCPH type 3 (MCPH3)	2
1.4 CDK5RAP2	3
1.5 MCPH3 animal models	3
2. Aims	4
3. Methodology	5
3.1 Mice	5
3.2 Histology and immunofluorescence staining	5
3.3 Cell cycle progression analysis	6
3.4 Golgi staining, dendritic complexity and spine analysis	6
3.5 Electrophysiology on <i>ex-vivo</i> brain slices	7
3.6 Imaging	8
3.7 Statistical analysis	8
4. Results	9
4.1 Hypomorphic gross phenotype and embryonic lethality	9
4.2 Microcephaly with thin neocortex and increase of superficial cortical layers relative cell density	9
4.3 Reduction in the dendritic complexity of layer II-III pyramidal neurons	10
4.4 Increase of layer II-III neuronal activity	10
4.5 Sterility in male mice	12
4.6 Lack of germ cells in <i>an/an</i> is due to an early developmental defect	13
4.7 Cdk5rap2 is required for normal germ cell cycle progression	13
5. Discussion	15
6. References	17

7. Affidavit + detailed statement of originality	21
8. Declaration of any eventual publications	22
8.1 Loss of CDK5RAP2 affects neural mESC differentiation	24
8.2 Golgi-Cox staining	38
8.3 Germ cell depletion in <i>an/an</i>	45
9. Curriculum Vitae	52
10. Complete list of publications	53
11. Acknowledgements	54

Figures

Figure 1. Illustration of the brain phenotype in MCPH patients and the main roles of MCPH proteins	2
Figure 2. Microcephaly with thin neocortex and increase of superficial cortical layers relative cell density	10
Figure 3. Layer II-III pyramidal neurons in <i>an/an</i> mice had reduced dendritic complexity, increased spine density	11
Figure 4. Testes of <i>Cdk5rap2</i> mutant mice lack germ cells	12
Figure 5. Schematic model of mechanism leading to embryonic loss of germ cells in <i>Cdk5rap2</i> mutant mice	14

Abstract

Patients with biallelic mutations in the Cyclin-dependent kinase 5 regulatory subunit-associated protein 2 (*CDK5RAP2*) gene suffer from autosomal recessive primary microcephaly type 3 (MCPH3) and intellectual disability at birth. Microcephaly is due to a reduction of brain volume which affects disproportionately the grey matter. *Cdk5rap2* mutant or *Hertwig's anemia* mice (*an/an*) have small brains and thin cortices already at early stages of neurogenesis. *Cdk5rap2* is a centrosomal protein highly expressed in the neural progenitor pool. Although the microcephaly phenotype in *an/an* has been explained by many mechanisms, the exact effect of a loss of *Cdk5rap2* function on neurogenesis and neuronal differentiation is not known. On the other hand, *Cdk5rap2* is expressed in various tissues, and, thus, other organs in *an/an* might be affected as well. Indeed, *an/an* males are infertile secondary to a severe germ cell deficiency. However, the mechanisms behind germ cell loss have not been studied before.

The aim of my PhD project was to improve our understanding of the role of *Cdk5rap2*. First, we aimed to analyse the effects of a loss of *Cdk5rap2* function on neurogenesis and on the differentiation of neocortical neurons in *an/an*. Second, the expression pattern of *Cdk5rap2* and the germline defect in *an/an* prompted us to further analyse the germline development in these mice. In order to study the phenotype of neocortical neurons in *an/an*, we applied a modified Golgi-Cox staining protocol. We detected a reduction in the dendritic complexity but an increase in the spine density of layer II-III pyramidal neurons in *an/an* mice when compared to wild type (+/+) littermates. Electrophysiological analysis showed an increase in layer II-III pyramidal neurons mEPSC frequency already at the beginning of synaptogenesis in (P6/7) *an/an* as a possible correlate for epilepsy in some patients with MCPH. In addition, we reported a critical role of *Cdk5rap2* in maintaining the germ cell pool. We found that infertility in *an/an* is due to an early developmental defect in the germ cells through mitotic delay, prolonged cell cycle and apoptosis.

We highlight that a neuronal differentiation defect, especially in the upper cortical layers, contributes to the microcephaly phenotype in MCPH. We also show that *Cdk5rap2*

plays a major role in maintaining the germ cell pool during development. Understanding the cause leading to infertility is likewise important for understanding the fate of neural progenitors and thus mechanisms leading to microcephaly in MCPH.

Zusammenfassung

Biallele Mutationen im Cyclin-dependent kinase 5 regulatory subunit-associated protein 2 Gen (*CDK5RAP2*) verursachen die Autosomal rezessive primäre Mikrozephalie Typ 3 (MCPH3). Patienten mit MCPH3 weisen eine schwere Mikrozephalie bei Geburt und eine Intelligenzminderung auf. Die Mikrozephalie ist auf eine Reduktion des Hirnvolumens zurückzuführen, die überproportional die graue Substanz betrifft. *Cdk5rap2* mutante Mäuse oder Hertwig Anämie Mäuse (*an/an*) haben bereits im frühen Stadien der Neurogenese kleine Gehirne und dünne Kortizes. *Cdk5rap2* ist ein zentrosomales Protein, das im neuronalen Vorläuferpool exprimiert wird. Obgleich einige potentielle Mechanismen, die zur Mikrozephalie der *an/an*-Mäuse beitragen, publiziert worden sind, ist der genaue Effekt eines Verlustes der Funktion von *Cdk5rap2* auf die Neurogenese und die neuronale Differenzierung nicht bekannt. Darüber hinaus wird *Cdk5rap2* in verschiedenen Geweben exprimiert, was eine Beteiligung weiterer Organe vermuten lässt. In der Tat sind *an/an*-Männlichen als Folge eines Verlustes ihrer Keimzellen unfruchtbar. Auch in diesem Fall sind die zugrundeliegenden Mechanismen unklar.

Ziel meines Dissertationsprojekts war es, das Verständnis für die Funktion von *Cdk5rap2* zu verbessern. Zunächst zielten wir darauf ab, die Auswirkungen eines Verlustes von *Cdk5rap2* auf die Neurogenese und die Differenzierung neokortikaler Neurone in *an/an*-Mäusen zu analysieren. Um den Phänotyp neokortikaler Neuronen in *an/an*-Mäusen zu untersuchen, wurde ein modifiziertes Golgi Cox-Färbeprotokoll angewendet. Wir fanden eine Verringerung der dendritischen Komplexität, aber eine höhere Dichte an Spines der Neurone in der Rindenschicht II-III in *an/an*-Mäusen im Vergleich zu Wildtypen (+/+). Darüber hinaus detektierten wir, mittels elektrophysiologischer Untersuchungen, bereits bei Beginn der Synaptogenese eine Zunahme der mEPSC-Frequenz der Neurone in der Rindenschicht II-III in den mutanten Mäusen. Letztere kann ein Korrelat für die bei einigen Patienten mit MCPH beschriebene Epilepsie darstellen. In einem weiteren Teil meines Projekts veranlasste uns das Expressionsmuster von *Cdk5rap2* und der Keimbahndefekt in *an/an*-Mäusen dazu, die Keimbahnentwicklung bei diesen Mäusen weiter zu analysieren. Wir fanden, dass die Infertilität der *an/an*-Mäuse auf einen frühen Entwicklungsdefekt in den

Keimzellen durch eine Verzögerung der Mitose, einen verlängerten Zellzyklus und Apoptose zurückzuführen ist.

In meiner Dissertationsarbeit konnte ich somit zusammenfassend zeigen, dass ein neuronaler Differenzierungsdefekt, insbesondere in den oberen kortikalen Schichten, zum Mikrozephalie Phänotyp bei MCPH3 beiträgt. Ich konnte zudem zeigen, dass Cdk5rap2 eine wichtige Rolle bei der Erhaltung des Keimzellpools während der Entwicklung innehat. Das Verständnis der Ursache für die Infertilität ist potentiell entscheidend für das Verständnis von Mechanismen, die zu Mikrozephalie in MCPH führen.

1. Introduction

1.1 Autosomal recessive primary microcephaly (MCPH)

Microcephaly is a clinical sign of small cranium with a significant reduction in the occipito-frontal head circumference (OFC) for more than two to three standard deviations (SD) below the mean for age, sex, and ethnicity. Microcephaly can be caused by environmental or genetic factors and is referred to as primary if it becomes apparent congenitally or secondary when it develops postnatally. Autosomal recessive primary microcephaly (**MicroC**ephal**y P**rim**ary H**ereditary; MCPH) is a rare neurodevelopmental disorder which has a prevalence of 1:30,000 to 1:250,000 live births (1). It is characterized by intellectual disability and microcephaly at birth due to severe reduction in brain volume (affecting disproportionately the neocortex) (2,3) (**Fig. 1**). Many patients suffer from hyperactivity, and some have epilepsy (2). So far, seventeen genes have been linked to MCPH world-wide and are referred to as MCPH1-MCPH17. Most MCPH proteins localize to the centrosome and the pericentriolar matrix. Most MCPH gene mutations lead to the production of non-functional, truncated proteins (2,4).

1.2 MCPH pathomechanisms

MCPH is currently acknowledged as a model disorder for an isolated brain phenotype. The microcephaly phenotype has been linked for long time to a stem cell defect with premature shift from symmetric to asymmetric progenitor cell divisions, leading to premature neurogenesis, a depletion of the progenitor pool and a reduction of the final number of neurons (2,5-7). In this line, a shift of the cleavage plane is likely not the only underlying mechanism as some MCPH mouse models - where the cleavage plane is unaffected - still show microcephaly (8,9). Additional studies also linked microcephaly phenotype to defects in chromosome condensation, microtubule dynamics, cell cycle checkpoint control and/or DNA damage-response signaling during embryonic neurogenesis (reviewed in (3,10)) (**Fig. 1**). Our research group also reported that the depletion of *Cdk5rap2* in murine embryonic stem cell (mESC) leads to a reduced propagation and survival of neural progenitors (11). More recently, it has been shown that mitotic delay in the neuronal progeny that leads to increase apoptosis is the major cause of microcephaly phenotype in *Magoh*^{+/-} mutant mouse model (12).

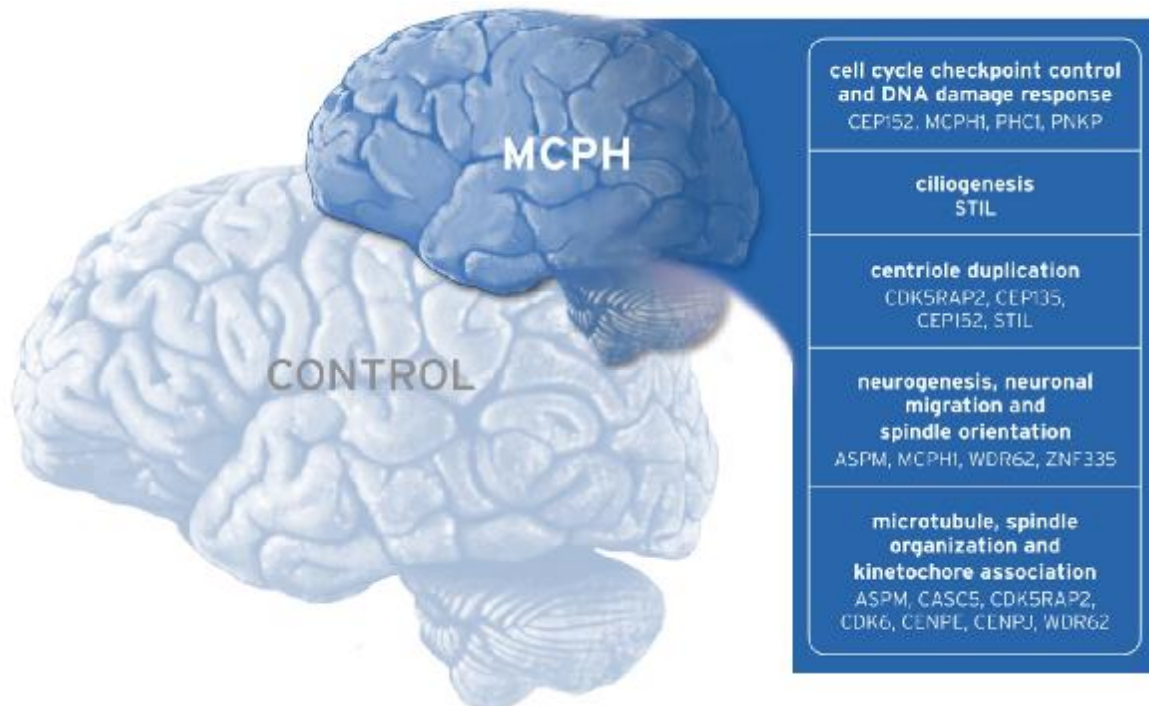


Figure 1. Illustration of the brain phenotype in MCPH patients and the main roles of MCPH proteins. Note the typical reduction in the brain volume and the simplification in cortical gyration of an otherwise architecturally normal brain. MCPH proteins are involved in cell cycle dynamics, ciliogenesis, the centrosome, neurogenesis, and neuronal migration.

1.3 MCPH type 3 (MCPH3)

Biallelic mutations in the Cyclin-dependent kinase 5 regulatory subunit-associated protein 2 (*CDK5RAP2*) gene cause MCPH type 3 (13,14). Currently there are five identified *CDK5RAP2* mutations in three Pakistani families, one Italian family and one Somali child: (i) a nonsense mutation in exon 4 (c.246T>A, p.Y82X) introducing a new splice acceptor site (14,15), (ii) a mutation in intron 26 (IVS26-15A>G, R1334SfsX5) resulting in a premature stop codon (14), (iii) a nonsense mutation in exon 8 (c.700G>T, p.E234X) introducing a frame shift (16), (iv) a nonsense mutation in exon 30 (c.4441C>T, p.R1481X) (17) and (v) a heterozygous mutation introducing a frame shift and a splicing respectively (c.524_528del and c.4005-1 G>A) (18).

1.4 CDK5RAP2

The human *CDK5RAP2* gene, composed of 38 exons, encodes 1893 amino acid protein. CDK5RAP2 full length protein contains an N-terminal interaction site with the gamma-tubulin ring complex (γ TuRC), a C-terminal interaction site with CDK5 regulatory subunit 1 (CDK5R1) interacting domain and several coiled-coil domains. Ortholog genes with similar domain structures are also found in other model organisms such as apes, cows, dogs, rats, mice and chicken (for review, see (3)).

Cdk5rap2 is highly expressed in the neural progenitor pool and its loss results in a depletion of apical progenitors and increased cell-cycle exit leading to premature neuronal differentiation (6). Other studies have shown that Cdk5rap2 plays roles in the cleavage plane orientation of apical progenitors (7), the maintenance of the centriole engagement and cohesion (19), the microtubule organizing function of the centrosome through interaction with the gamma tubulin ring complex (γ TuRC; (20)) and the proper spindle formation and chromosome segregation (14). Moreover, our research group found intriguing concordance between regions of high Cdk5rap2 expression in the mouse and sites of pathology suggested by neuroimaging in humans and from mouse studies (21). These findings in human tissue confirm those in mouse tissues, underlining the function of CDK5RAP2 in cell proliferation and arguing for a conserved role of this protein in the development of the mammalian cerebral cortex.

1.5 MCPH3 animal models

Cdk5rap2 mutant or *Hertwig's anemia* mice (*an/an*), which arose from a heavily irradiated mouse, were previously known solely for their hematopoietic phenotype (macrocytic, hypoproliferative anemia, leucopenia) (22). The *an/an* males are infertile secondary to a severe germ cell deficiency, and *an/an* females cannot deliver pups (23). Additionally, high level of abnormal chromosome number (aneuploidy) has been reported in these mice (24). Recent identification of an exon 4 inversion in *an/an Cdk5rap2* gene led to their neurological assessment and their identification as an MCPH3 model (7). *Cdk5rap2* is highly expressed in the neural progenitor pool, and *an/an* have small brains and thin cortices already at early stages of neurogenesis during embryonal development (6,7).

Drosophila embryos mutant for the *Cdk5rap2* homologous gene centrosomin (*cnn*^{-/-}) are viable, and only subtle defects of asymmetric divisions occurred in *cnn* mutant neuroblasts (no reduction of brain size) (25,26). It has been illustrated that *cnn* is required for centrosome cohesion and for docking of the γ TuRC to the centrosome via its N-terminal domain (25,27).

2. Aims

In the first part of my PhD thesis project, we analyzed the effects of a loss of *Cdk5rap2* function on neurogenesis and on the differentiation of neocortical neurons in *an/an* as a mouse model of MCPH3. For this, we applied Nissl and several immunohistochemistry staining methods on brain sections of both wild type (+/+) and *an/an* mice. We also succeeded in applying our modified protocol of Golgi Cox staining (28) to detect possible changes in dendritic complexity of layer II/III neocortical neurons. In collaboration with Prof. Dr. Christian Rosenmund, NeuroCure, Charité, neuronal excitation-inhibition and circuitry formation in mixed-cerebral *in-vitro* cultures from +/+ and *an/an* mice were analysed. In addition, the neurons of layer II/III in *ex-vivo* brain samples were patched and studied for the neuronal activity at postnatal day 6/7 (P6/P7) and at adult ages in collaboration with PD Dr. Ulf Strauss, Institute for Cell Biology and Neurobiology, Charité. This was particularly intriguing as smaller brain volume does not necessarily correlate with IQ and MCPH patients suffer from hyperactivity and epilepsy.

The expression pattern of *Cdk5rap2* and the germline defect in *an/an* prompted us to further analyse the germline development in these mice in a second part of my PhD thesis project. We studied +/+ and *an/an* testis samples from both postnatal day 0 (P0) and adult (P53-P79) mice. As we found a severe phenotype defect at P0 age, we then studied embryonic sections of *an/an* mice at the level of the testes and the genital ridges at embryonal day 14.5 (E14.5) and E12.5 respectively. To further investigate the fate of the germ cells in *an/an* mice, we analyzed their proliferation and apoptosis behavior at E11.5 and E12.5.

3. Methodology

3.1 Mice

an/an carrying an inversion of exon 4 (that leads to exon skipping;(7)) were generated by crossing heterozygous (+/*an*) mice (*C57BL/6* background; Jackson lab, Stock No: 002306). Genotyping was confirmed by PCR primers for (+/+) F 5'-TC ACT GAG CTG AAG AAG GAG AA-3', R 5'-TGT CTT TCT GCC CTG ACA GT-3' and (*an/an*) F 5'-GC AAT CAC TAA AAT GTC CGA TT-3', R 5'-TGT CTT TCT GCC CTG ACA GT-3' with an expected 1047 bp band in (+/+), a 500 bp band in (*an/an*) and both bands in (+/*an*). All mouse experiments were carried out in accordance to the national ethic principles (registration no. T0309/09).

3.2 Histology and immunofluorescence staining

After dissection, brains were fixed in paraformaldehyde (PFA; 4%) for overnight, dehydrated in an ethanol series (50, 70, 85, 90, 100%), cleaned with xylene and embedded in paraffin. The *tunicae albuginea* of adult testes was punctured with a needle to allow rapid penetration of the fixative. At E12.5 and E14.5, whole embryos were used. Following fixation in 4% PFA for 10 min (P0), 4 h (adult), or overnight (E12.5, E14.5), testes and embryos were processed as described above. 10 µm brain sections and 5 µm testis/embryos were then cut on a microtome and collected on Superfrost plus slides®.

Paraffin sections were deparaffinized, exposed to heat-mediated antigen retrieval citrate-based solution (pH 6.0; H-3300, Vector Laboratories, USA), blocked for 1 hour with 10% donkey or goat normal serum at room temperature (RT) and incubated overnight with the primary antibody at RT followed by an incubation with the corresponding secondary antibodies for 2 hours at RT in dark. The following primary antibodies were used at the specified dilutions: rabbit anti-Cux1 (1:200; Santa Cruz Biotechnology, Heidelberg, Germany, sc-13024), rat anti-Ctip2 (1:250; Abcam, Cambridge, UK, ab18465), mouse anti-parvalbumin (PV, 1:2000; Swant, Switzerland, PV 235), guinea pig anti-vesicular glutamate transporter 1 (vGlut1, 1:500; Merck-Millipore, Germany, AB5905), rabbit anti-post synaptic density 95 (PSD95, 1:200; Synaptic System, Göttingen, Germany, 124-002), rabbit anti-mouse vasa homolog (MVH/DDX4, 1:500; Abcam, Cambridge, UK, ab13840), rat anti-germ cell-specific antigen (TRA98, 1:500; Abcam, ab82527), mouse anti-phospho-histone H3 (pH3, 1:100; Cell Signaling, Frankfurt, Germany, 9706), rabbit anti-activated cleaved

Caspase 3 (1:200, Cell Signaling, 9661), mouse anti-5-Bromo-2'-deoxyuridine (BrdU, 1:300; Millipore, MAB3424, clone AH4H7-1) and rat anti-BrdU (1:250; Abcam, ab6326). Secondary antibodies (1:400) were goat Alexa Fluor® 488 conjugate anti-mouse IgG, goat Alexa Fluor® 488 conjugate anti-rabbit IgG, donkey Alexa Fluor® 488 conjugate anti-rat and anti-guinea pig IgG (Invitrogen, Darmstadt, Germany), goat Cy3-conjugate anti-rat IgG (Invitrogen, Darmstadt, Germany) donkey Cy3-conjugated anti-rabbit IgG (Jackson ImmunoResearch, Suffolk, UK). Nuclei were stained with 40,6-diamidino-2-phenylindole (DAPI, 1:1000, Sigma-Aldrich, USA).

P0 and adult testis sections at the position of maximal testis diameter were also deparaffinized and stained with Hematoxylin and Eosin staining (H&E). Deparaffinized coronal brain sections at the same level of corpus callosum and anterior commissure were stained with cresyl violet staining (Nissl). Measurements of testis diameter, parietal cortical thickness and of neocortical area were carried out using ImageJ software.

3.3 Cell cycle progression analysis

Cell cycle progression study in the *+/+* and *an/an* mice was performed by successive pulse labeling of heterozygous (*an/+*) pregnant mice at E11.5 with two different thymidine analogs: 5-Iodo-2'-deoxyuridine (Iddu) and 5-Bromo-2'-deoxyuridine (BrdU, interval 4 hours). 30 minutes after the second pulse, the E11.5 embryos were collected and double immunostained with Rat anti-BrdU (which detects both Iddu and BrdU labeled cells) and Mouse anti-BrdU (which specifically detects BrdU labeled cells).

3.4 Golgi staining, dendritic complexity and spine analysis

Golgi-Cox impregnation for *+/+* and *an/an* adult brain samples was performed according to our published protocol (28). Briefly, brains were cut into two halves, immersed in the impregnation solution in darkness at room temperature (RT) for 2 weeks and transferred into tissue-protectant solution at 4 °C for 4 days. Brains were then cut into 200 µm for dendritic complexity analysis and 100 µm for dendritic spine analysis. Sections were collected on gelatin-coated slides, left to dry for two days, developed, dehydrated through ethanol series, cleared in xylol solution and mounted in Eukitt (quick-252 hardening mounting medium; 03989, Fluka analytical, Germany).

For dendritic complexity assessment, Sholl analysis (29) was performed for layer II-III pyramidal neurons of matched *+/+* and *an/an* neocortical regions. The total intersection number of the dendritic tree with 30 10- μ m spaced concentric circles were counted with cell counter plug-in available for ImageJ. Simple neurite tracer plug-in available for Fiji/ImageJ was used to draw representative neurons. The number of spines was counted in 20 μ m long segments of secondary dendrites using ImageJ. Spines were classified in to one of three morphological subtypes: mushroom which have a large bulbous end, stubby which have no neck and thin-shaped which have long neck.

3.5 Electrophysiology on *ex-vivo* brain slices

Slices of mouse brains (P6/7 and adult) were used for *ex vivo* recordings. After deep anesthesia with isoflurane, mice were decapitated, brains removed and transferred to ice-cold artificial cerebrospinal fluid (ACSF). Coronal slices (300 μ m nominal thickness) containing the somatosensory cortex were cut on a Leica VT1200 (Leica Microsystems, Germany). Slices recovered for 30 minutes at 34 °C and were kept at room temperature afterwards.

Somatic whole-cell recordings were performed in a submerged recording chamber perfused with ACSF. Pyramidal neurons were identified in upper layers (II-III) using an upright microscope equipped with infrared differential interference contrast optics (Axioskop FS2; Zeiss or Olympus BX51, Germany) and approached with patch pipettes (tip resistance 3 - 5 M Ω). Only neurons with resting potentials below -65 mV and spiking characteristics of principal neurons were considered. Spontaneous postsynaptic currents (sPSC) were recorded in continuous voltage clamp at a holding potential of -60 mV. Miniature excitatory postsynaptic currents (mEPSC) represent AMPA mediated currents (30). Paired EPSCs (50 ms interval) were elicited by square pulse (100 μ s) stimulation of the slice 50 -100 μ m lateral of the recording electrode at the border between layer II-III and IV with a concentric tungsten electrode (TM33CCINS, WPI, USA).

Data from patch-clamp recordings were collected with an EPC-10 double amplifier (HEKA, Germany), digitized (10 kHz, after Bessel filtering at 2.9 kHz) and stored using PatchMaster software (HEKA). Events were detected offline using Mini Analysis Program (Synptosoftware Inc., USA).

3.6 Imaging

The brightfield images were taken by Olympus BX60 microscope equipped with an AxioCam MRc Zeiss camera and Axiovision 4.8 software (Zeiss, Göttingen, Germany). For studying dendritic arborization, 1- μ m-spaced Z-stack brightfield images were taken by Olympus IX81 microscope equipped with a F View II (sw) camera (Soft Imaging System GmbH, Münster, Germany).

Fluorescent images were taken by Olympus BX51 microscope by an Intas camera and Magnafire 2.1B software (Olympus, Hamburg, Germany) and lsm5exciter Zeiss confocal microscope with the software Zen (version 2009, Zeiss, Jena, Germany). All images were processed using Adobe Photoshop CS6 version 13.0x64 and Fiji/ImageJ software.

3.7 Statistical analysis

For *in vivo* parietal cortical thickness, neocortical area, cortical layers, Scholl analysis and spine density statistics, two-tailed Students' t tests were applied. Statistics of *ex-vivo* brain slices electrophysiology were performed using Origin8.5 (OriginLab, USA). For normal distributed datasets (Shapiro-Wilk test) two tailed Student's t-tests was used. In the case of significant deviations from normal distribution ($p \leq 0.05$) the non-parametric Mann-Whitney-U test was used. For comparing probability distributions the Kolmogorov-Smirnov test was used.

Data of dissociated cell cultures were first tested for a Gaussian distribution with D'Agostino and Pearson omnibus normality test. If the data passed the normality test, one-way ANOVA followed by Bonferroni multiple-comparison tests were performed. Otherwise, nonparametric Kruskal-Wallis test followed by Dunn multiple comparison tests were used.

4. Results

4.1 Hypomorphic gross phenotype and embryonic lethality

The *an/an* mice can be recognized by their characteristic hypomorphic gross phenotype apparent at birth. While the expected Mendelian ratio of *an/an* mice was found at embryonic days E12.5-E14.5 (*an/an* : *an/+* : *+/+* = 24 : 43 : 16), only 9.5% of the offspring carried a homozygous mutant genotype (*an/an*) at P0 (*an/an* : *an/+* : *+/+* = 46 : 287 : 152), indicating *in utero* lethality.

4.2 Microcephaly with thin neocortex and increase of superficial cortical layers relative cell density

We first studied the general brain architecture in postnatal day 0 (P0) and adult Nissl-stained *an/an* brain sections. We found that the overall brain size, neocortical area and parietal cortical thickness are significantly reduced in the *an/an* mice when compared to the *+/+* littermates (**Fig. 2**). Apart for the general reduction in size, brain structures were normal (**Fig.2A**). We then studied the cortical layer organization in the *an/an* using immunostaining with Cux1 (layers II–IV) and Ctip2 (layers V–VI) markers. We found that the total DAPI⁺ nuclei, Cux1⁺ and Ctip2⁺ cortical neurons per view-field at P0 and adult *an/an* mice are significantly reduced in *an/an* mice. However, the relative number of both layer populations with respect to total DAPI⁺ nuclei is not changed. While both Cux1⁺ superficial layers and Ctip2⁺ deepest layers are thinner, only the relative thickness of superficial layers is significantly reduced in P0 and adult *an/an* mice. These findings point towards a reduction in the space between superficial cortical layer neurons reflected by an increase in the relative density.

Next, we checked for interneuron pool in *an/an* brain sections. Using PV as an interneuron marker, we found that the number of interneurons positive for PV per view-field is reduced in the adult *an/an* mice while the percentage of these cells in relation to total DAPI⁺ nuclei per view-field is not changed. Together, these data emphasize that the increase of superficial cortical layers relative density in *an/an* mice is rather due to a potential defect in neuronal differentiation.

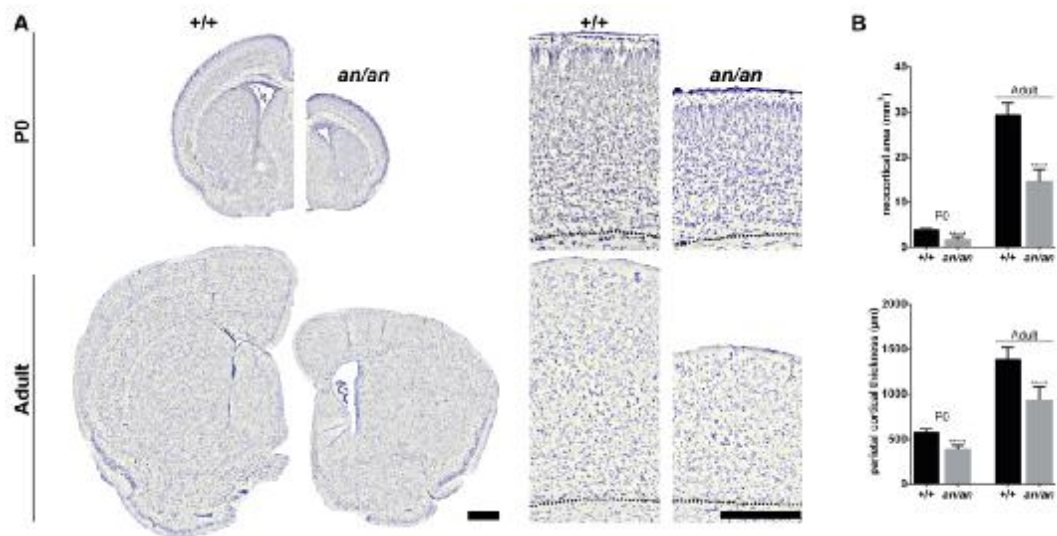


Figure 2. Microcephaly with thin neocortex and increase of superficial cortical layers relative cell density. (A) Coronal brain sections of P0 and adult littermate animals with parietal cortices magnified on the right (Nissl staining, DIC images, scale bars 500 μm). **(B)** Significant reduction of the neocortical area and parietal cortical thickness in *an/an* mice ($n=7$ animals/group). Error bars indicate s.d. Students' t test: **** $p<0.0001$.

4.3 Reduction in the dendritic complexity of layer II-III pyramidal neurons

To study neuronal differentiation in *an/an* mice, we applied Golgi staining method on adult mouse brains. Using Sholl analysis (29), we counted the number of dendrite intersections for concentric circles, centred at the cell body, of gradually increasing radius, up to a distance of 300 μm from the soma, to study individual neurons from both +/+ and *an/an* samples. This analysis, which quantifies the dendritic complexity, showed a significantly reduced number of apical and basal dendritic intersections of layer II-III pyramidal neurons in the *an/an* mice compared to the +/+ littermates (**Fig. 3A,B**). This indicates that a neuronal differentiation defect in *an/an*, especially in the upper cortical layers, contributes to the microcephaly phenotype in this animal model of MCPH3.

4.4 Increase of layer II-III neuronal activity

The fact that MCPH patients often suffer from hyperactivity and some from epilepsy prompted us to study layer II-III dendritic spine and synaptic development as well as neuronal activity in *an/an*. For this, we analyzed dendritic spines in layer II-III Golgi-stained pyramidal neurons and found a significant increase in the number of spines with more thin-shaped

immature subtype in the *an/an* adult mice compared to the *+/+* (**Fig. 3C,D**). We then recorded sPSC of layer II-III pyramidal neurons in *ex-vivo* adult brain samples. The results showed an increase in the mEPSC frequency but no change in amplitude in the *an/an* when compared to the *+/+* littermates.

To further investigate neuronal activity in *an/an* mice, we analyzed layer II-III neuronal activity in *ex-vivo* P6/7 brain samples. At this age of early synaptogenesis, we found also an increase in the mEPSC frequency but no change in amplitude in the *an/an* mice when compared to the *+/+* littermates. In line with these electrophysiological data, we found more vGlut/PSD95 positive synapses, an indication of active synapses, in P6/7 *an/an* layer II-III neurons. Taken together, these results indicate an increase of layer II-III neuronal activity in *an/an* mice.

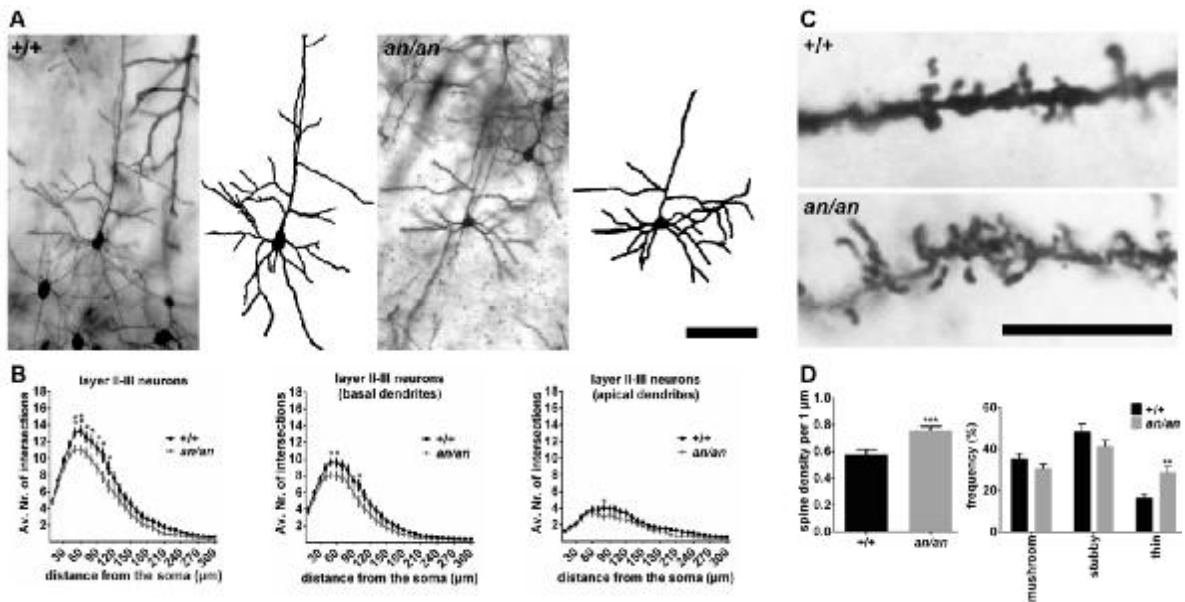


Figure 3. Layer II-III pyramidal neurons in *an/an* mice had reduced dendritic complexity, increased spine density. (A) Photomicrographs and reconstructed layer II-III pyramidal neurons from both *+/+* and *an/an* adult mice (Golgi staining, DIC images, scale bar 100 μm). (B) Scholl analysis plot of dendritic complexity. The average numbers of dendritic intersections with circles of 50-110 μm away from the soma are reduced in *an/an* mice (n= 44 *+/+* and 39 *an/an* neurons from 4-6 animals/group). (C) Segments of secondary basal dendrites of layer II-III pyramidal neurons from both *+/+* and *an/an* adult mice (Golgi staining, DIC images, scale bar 10 μm). (D) The average number of spines per 1 μm-long dendritic segments is significantly increased with more thin-shaped immature subtype in *an/an* mice (n= 410 *+/+* and 373 *an/an* spines counted in 34 *+/+* and 30 *an/an* 20 μm-long dendritic segments from 5 animals/group). Error bars indicate s.e.m. Students' t test: *p<0.05, **p<0.01, ***p<0.001.

4.5 Sterility in male mice

Testes of *an/an* mice at both P0 and adult ages were severely reduced in cross-sectional area, weight and testes/body weight ratio. Further analysis of H&E-stained testes revealed the absence of gonocytes in P0 *an/an* testes and of all spermatogenic cells from spermatogonia to mature sperms in adult *an/an* testes (**Fig. 4**). We further confirmed this by immunostaining, applying germ cell markers MVH and TRA98. The seminiferous tubules, demarked by Sertoli cells, were normal in architecture, but notably smaller in size in *an/an* mice due to lack of the germ cells.

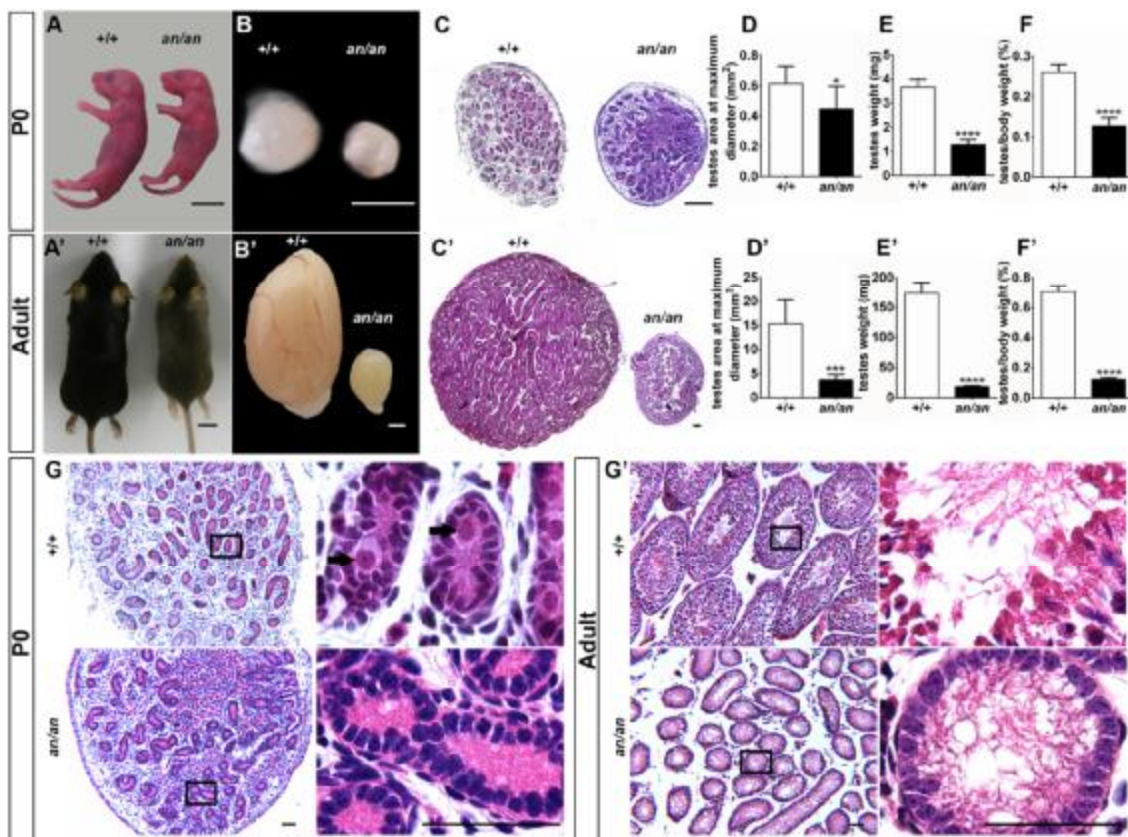


Figure 4. Testes of *Cdk5rap2* mutant mice lack germ cells. (A-B') Hypomorphic gross phenotype and reduced testis size of P0 and adult *an/an* mice. Scale bars: 10 mm (A, A') and 1 mm (B, B'). **(C-D')** Testis area is reduced in P0 and adult *an/an* mice at the position of maximal testis diameter. Scale bars 200 μ m, n=6-7 animals/group. **(E-F')** Reduction of testis weight and testis/body weight is already present at P0 in *an/an* mice and also significant in adult mice (n=3-6 (P0) and n=6-7 (adult) animals/group). **(G-G')** Absence of gonocytes (arrows) in seminiferous tubules at P0 and of spermatogenic cells in adult *an/an* mice. Scale bars 50 μ m, H&E staining, DIC images. Error bars indicate s.d., Students' t-test, * p <0.05, *** p <0.001 **** p <0.0001.

4.6 Lack of germ cells in *an/an* is due to an early developmental defect

The absence of germ cells in *an/an* males at P0 points towards an earlier developmental defect in the germline. For this, we studied embryonic sections of *an/an* mice at the level of the testes and the genital ridges at E14.5 and E12.5, respectively. At E14.5, testes of *an/an* mice lacked gonocytes positive for MVH or TRA98. Compared to wild type *+/+* mice, E12.5 *an/an* mouse sections showed a significantly reduced number of gonocytes/primordial germ cells (PGCs) in the genital ridge (**Fig. 5**). We could not detect any aberrant located cells, i.e. cells outside the vicinity of the genital ridges.

To further investigate the fate of the germ cells in *an/an* mice, we studied their proliferation and apoptosis behavior at E12.5. Here, more germ cells were positive for mitotic cell marker (pH3) in *an/an* compared to *+/+* mice. Further analysis of these mitotic cells revealed more pro/pro-metaphase cells in *an/an* compared to *+/+* mice. Using activated Caspase 3 as an apoptotic cell marker, we found a significant increase in apoptotic germ cells in *an/an* compared to *+/+* mice.

4.7 *Cdk5rap2* is required for normal germ cell cycle progression

We also checked germ cell cycle progression in the *an/an* mice by performing successive pulse labeling of heterozygous (*an/+*) pregnant mice at E11.5 with two different thymidine analogs: Iddu and BrdU (interval 4 hours). This enabled us to estimate the ratio of germ cells that left the cell cycle within a time frame of 4 hours. In E11.5 *+/+* embryos, we found many germ cells already exited the cell cycle after 4 hours as detected by exclusive positivity for Iddu ($54,49 \pm 3,2\%$). In *an/an* embryos, however, less germ cells had exited the cell cycle during the same time frame ($39,02 \pm 1,8\%$, $P < 0.01$).

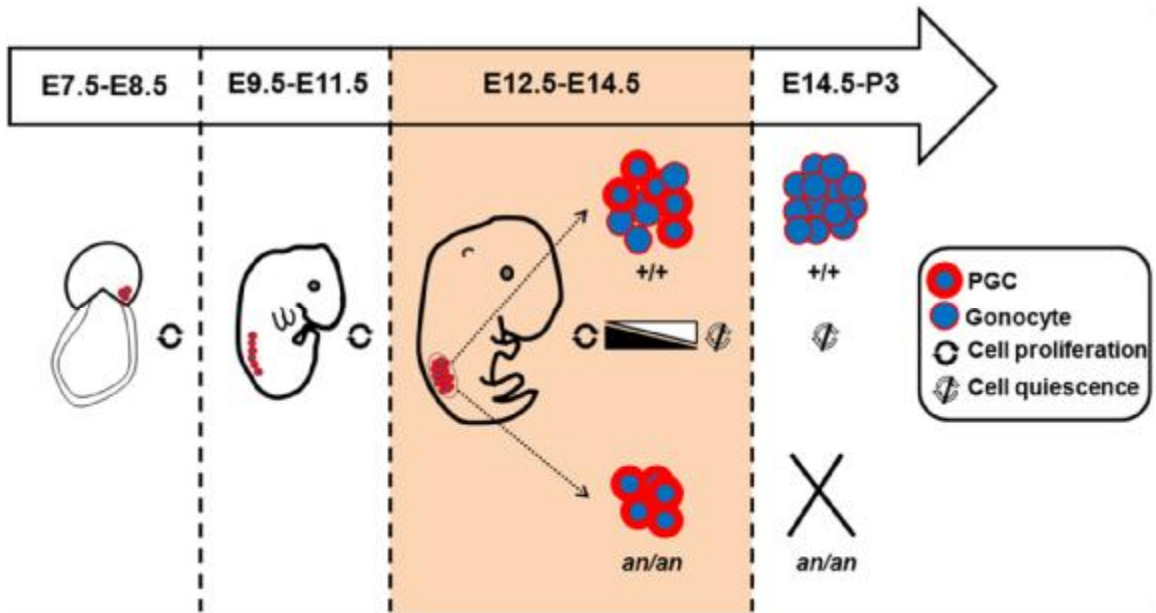


Figure 5. Schematic model of mechanism leading to embryonic loss of germ cells in *Cdk5rap2* mutant mice. Germ cells are specified at around E7.5, proliferate and migrate toward the genital ridge around E8.5-12.5 in mice. In *an/an* mice, germ cells undergo massive apoptosis at a time when the cells undergo physiologically mitotic arrest (E12.5-E14.5). This cumulates in a loss of germ cells during embryonic development, later apparent in male infertility.

5. Discussion

The formation of the mammalian cerebral cortex requires proliferation, migration, differentiation and connectivity of neurons. Any defect in one or more of these overlapping processes leads to a spectrum of congenital brain malformations. The microcephaly phenotype in MCPH has been linked for long time to a stem cell defect with a premature shift from symmetric to asymmetric progenitor cell divisions leading to premature neurogenesis, a depletion of the progenitor pool and a reduction of the final number of neurons (2,5-7). In my PhD thesis project, we observed that a neuronal differentiation defect also contributes to the microcephaly phenotype. This was demonstrated by a reduction in the adult *an/an* dendritic complexity of layer II-III pyramidal compared to the *+/+* (**Fig. 3**). Moreover, we found an increase in mEPSC frequency (but not amplitude) of these cells already at the beginning of synaptogenesis. Consistent with this, we showed an increase in the spine density of layers II-III pyramidal neurons in the adult *an/an* and number of vGlut/PSD95 positive synapses in the (P6/7) *an/an* compared to *+/+*. These data are in the line of clinical findings of some MCPH patients who suffer from hyperactivity and epilepsy (2).

Microcephaly has been in the focus of neuroscience for years and even more so in the last months due to the Zika virus epidemic (31). Most studies focused naturally on microcephaly-linked gene products and their role in brain development, largely neglecting their putative functions in the development of other organs. However, *Cdk5rap2* is ubiquitously expressed (21) and exerts functions such as maintaining centrosome function, spindle assembly and orientation and/or cell cycle checkpoint control (3,32). In my PhD thesis project, we highlight the critical role of *Cdk5rap2* in maintaining the germ cell pool. We demonstrate infertility secondary to a loss of spermatogenic cells in adult mice.

Normally, germ cells in mice are specified at E6.25–7.25, proliferate and migrate toward the genital ridge at E8.5-12.5 and undergo mitotic arrest at E12.5-E14.5 in males (33-35). The current availability of germ cell markers and the advantage of immunohistochemistry technique allowed us to explore the exact time period when these cells are lost in *an/an* during development. We show that germ cells in *an/an* are already significantly reduced in number at E12.5 and lost by E14.5 (**Fig. 5**). The increase in the relative number of mitotic germ cells in E12.5 *an/an* mice with more cells in pro/pro-metaphase and a lower total number of germ cells indicate a delay in mitotic progression of

these cells. Intriguingly, loss of *Cdk5rap2* mutant germ cells in *an/an* mice occurs at a time when these cells physiologically exit the cell cycle and enter a mitotic quiescent phase. Using successive pulse labeling technique for proliferative germ cells, we also found that less *an/an* germ cells had exited the cell cycle compared to the *+/+*. The lack of germ cells in an aberrant location at E12.5 renders abnormal migration an unlikely cause of germ cell depletion in *an/an* mice. The normal architecture of testicular somatic cells, Sertoli and Leydig cells, suggests that these cells play no major role in *an/an* germ cell phenotype (**Fig. 4**).

Our results suggest increased apoptosis as a consequence of mitotic delay as the likely cause of *Cdk5rap2* mutant germ cell depletion. This is in line with recent studies linking mitotic delay to increased apoptosis of neuronal progeny (12) as well as evidence stressing apoptosis as a critical regulator of the germ cell pool (36). In agreement with a germ cell defect in the MCPH3 mouse model, a severe reduction in testis volume due to a massive loss of germ cells has been reported in a mouse model of MCPH5 (8). The underlying pathomechanism may be similar to that reported here in the MCPH3 mouse model.

Understanding the cause leading to infertility is likewise important for understanding the fate of neural progenitors and thus mechanisms leading to microcephaly in MCPH. Further studies in humans are warranted to analyze the significance of these findings for individuals with biallelic *CDK5RAP2* gene mutations.

6. References

1. Van Den Bosch J. Microcephaly in the Netherlands: a clinical and genetical study. *Ann Hum Genet* 1959;23:91-116.
2. Kaindl AM, Passemard S, Kumar P, Kraemer N, Issa L, Zwirner A, Gerard B, Verloes A, Mani S, Gressens P. Many roads lead to primary autosomal recessive microcephaly. *Progress in Neurobiology* 2010;90:363-83.
3. Kraemer N, Issa L, Hauck SCR, Mani S, Ninnemann O, Kaindl AM. What's the hype about CDK5RAP2? *Cellular and Molecular Life Sciences* 2011;68:1719-36.
4. Barbelanne M, Tsang WY. Molecular and cellular basis of autosomal recessive primary microcephaly. *Biomed Res Int* 2014;2014:547986.
5. Fish JL, Kosodo Y, Enard W, Pääbo S, Huttner WB. Aspm specifically maintains symmetric proliferative divisions of neuroepithelial cells. *Proceedings of the National Academy of Sciences of the United States of America* 2006;103:10438-43.
6. Buchman JJ, Tseng HC, Zhou Y, Frank CL, Xie Z, Tsai LH. Cdk5rap2 interacts with pericentrin to maintain the neural progenitor pool in the developing neocortex. *Neuron* 2010;66:386-402.
7. Lizarraga SB, Margossian SP, Harris MH, Campagna DR, Han AP, Blevins S, Mudbhary R, Barker JE, Walsh CA, Fleming MD. Cdk5rap2 regulates centrosome function and chromosome segregation in neuronal progenitors. *Development* 2010;137:1907-17.
8. Pulvers JN, Bryk J, Fish JL, Wilsch-Bräuninger M, Arai Y, Schreier D, Naumann R, Helppi J, Habermann B, Vogt J, Nitsch R, Tóth A, Enard W, Pääbo S, Huttner WB. Mutations in mouse Aspm (abnormal spindle-like microcephaly associated) cause not only microcephaly but also major defects in the germline. *Proceedings of the National Academy of Sciences of the United States of America* 2010;107:16595-600.
9. Fietz SA, Huttner WB. Cortical progenitor expansion, self-renewal and neurogenesis—a polarized perspective. *Current opinion in neurobiology* 2011;21:23-35.
10. Mahmood S, Ahmad W, Hassan MJ. Autosomal recessive primary microcephaly (MCPH): Clinical manifestations, genetic heterogeneity and mutation continuum. *Orphanet Journal of Rare Diseases* 2011;6:39-54.

11. Kraemer N, Ravindran E, Zaqout S, Neubert G, Schindler D, Ninnemann O, Graf R, Seiler AE, Kaindl AM. Loss of CDK5RAP2 affects neural but not non-neural mESC differentiation into cardiomyocytes. *Cell Cycle* 2015;14:2044-57.
12. Pilaz LJ, McMahon JJ, Miller EE, Lennox AL, Suzuki A, Salmon E, Silver DL. Prolonged Mitosis of Neural Progenitors Alters Cell Fate in the Developing Brain. *Neuron* 2016;89:83-99.
13. Moynihan L, Jackson AP, Roberts E, Karbani G, Lewis I, Corry P, Turner G, Mueller RF, Lench NJ, Woods CG. A third novel locus for primary autosomal recessive microcephaly maps to chromosome 9q34. *American Journal of Human Genetics* 2000;66:724-7.
14. Bond J, Roberts E, Springell K, Lizarraga S, Scott S, Higgins J, Hampshire DJ, Morrison EE, Leal GF, Silva EO, Costa SMR, Baralle D, Raponi M, Karbani G, Rashid Y, Jafri H, Bennett C, Corry P, Walsh CA, Woods CG. A centrosomal mechanism involving CDK5RAP2 and CENPJ controls brain size. *Nature Genetics* 2005;37:353-5.
15. Hassan MJ, Khurshid M, Azeem Z, John P, Ali G, Chishti MS, Ahmad W. Previously described sequence variant in CDK5RAP2 gene in a Pakistani family with autosomal recessive primary microcephaly. *BMC Med Genet* 2007;8:58-65.
16. Pagnamenta AT, Murray JE, Yoon G, Akha ES, Harrison V, Bicknell LS, Ajilogba K, Stewart H, Kini U, Taylor JC, Keays DA, Jackson AP, Knight SJ. A novel nonsense CDK5RAP2 mutation in a Somali child with primary microcephaly and sensorineural hearing loss. *American Journal of Medical Genetics, Part A* 2012;158 A:2577-82.
17. Issa L, Mueller K, Seufert K, Kraemer N, Rosenkotter H, Ninnemann O, Buob M, Kaindl AM, Morris-Rosendahl DJ. Clinical and cellular features in patients with primary autosomal recessive microcephaly and a novel CDK5RAP2 mutation. *Orphanet Journal of Rare Diseases* 2013;8:59-73.
18. Tan CA, Topper S, Ward Melver C, Stein J, Reeder A, Arndt K, Das S. The first case of CDK5RAP2-related primary microcephaly in a non-consanguineous patient identified by next generation sequencing. *Brain and Development* 2013;36:351-5.
19. Barrera JA, Kao LR, Hammer RE, Seemann J, Fuchs JL, Megraw TL. CDK5RAP2 regulates centriole engagement and cohesion in mice. *Developmental Cell* 2010;18:913-26.

20. Fong KW, Choi YK, Rattner JB, Qi RZ. CDK5RAP2 is a pericentriolar protein that functions in centrosomal attachment of the γ -tubulin ring complex. *Molecular Biology of the Cell* 2008;19:115-25.
21. Issa L, Kraemer N, Rickert CH, Sifringer M, Ninnemann O, Stoltenburg-Didinger G, Kaindl AM. CDK5RAP2 expression during murine and human brain development correlates with pathology in primary autosomal recessive microcephaly. *Cerebral Cortex* 2013;23:2245-60.
22. Barker JE, Bernstein SE. Hertwig's anemia: characterization of the stem cell defect. *Blood* 1983;61:765-9.
23. Russell ES, McFarland EC, Peters H. Gametic and pleiotropic defects in mouse fetuses with Hertwigs macrocytic anemia. *Developmental Biology* 1985;110:331-7.
24. Eppig JT, Barker JE. Chromosome abnormalities in mice with Hertwig's anemia. *Blood* 1984;64:727-32.
25. Lucas EP, Raff JW. Maintaining the proper connection between the centrioles and the pericentriolar matrix requires *Drosophila* centrosomin. *J Cell Biol* 2007;178:725-32.
26. Megraw TL, Li K, Kao LR, Kaufman TC. The centrosomin protein is required for centrosome assembly and function during cleavage in *Drosophila*. *Development* 1999;126:2829-39.
27. Zhang J, Megraw TL. Proper recruitment of gamma-tubulin and D-TACC/Msps to embryonic *Drosophila* centrosomes requires Centrosomin Motif 1. *Mol Biol Cell* 2007;18:4037-49.
28. Zaqout S, Kaindl AM. Golgi-Cox Staining Step by Step. *Front Neuroanat* 2016;10:38-45.
29. Sholl DA. Dendritic organization in the neurons of the visual and motor cortices of the cat. *J Anat* 1953;87:387-406.
30. Schuster S, Rivalan M, Strauss U, Stoenica L, Trimbuch T, Rademacher N, Parthasarathy S, Lajko D, Rosenmund C, Shoichet SA, Winter Y, Tarabykin V, Rosario M. NOMA-GAP/ARHGAP33 regulates synapse development and autistic-like behavior in the mouse. *Molecular psychiatry* 2015;20:1120-31.
31. Kleber de Oliveira W, Cortez-Escalante J, De Oliveira WT, do Carmo GM, Henriques CM, Coelho GE, Araujo de Franca GV. Increase in Reported Prevalence of Microcephaly in

Infants Born to Women Living in Areas with Confirmed Zika Virus Transmission During the First Trimester of Pregnancy - Brazil, 2015. *MMWR Morbidity and mortality weekly report* 2016;65:242-7.

32. Megraw TL, Sharkey JT, Nowakowski RS. Cdk5rap2 exposes the centrosomal root of microcephaly syndromes. *Trends in Cell Biology* 2011;21:470-80.

33. De Felici M. Primordial germ cell biology at the beginning of the XXI century. *Int J Dev Biol* 2009;53:891-4.

34. McLaren A. Primordial germ cells in the mouse. *Developmental Biology* 2003;262:1-15.

35. Western PS, Miles DC, van den Bergen JA, Burton M, Sinclair AH. Dynamic regulation of mitotic arrest in fetal male germ cells. *Stem Cells* 2008;26:339-47.

36. Aitken RJ, Findlay JK, Hutt KJ, Kerr JB. Apoptosis in the germ line. *Reproduction* 2011;141:139-50.

7. Affidavit + detailed statement of originality

I, Sami Zaqout, certify under penalty of perjury by my own signature that I have submitted the thesis on the topic „Cyclin-dependent kinase 5 regulatory subunit-associated protein 2 (Cdk5rap2) in neuronal differentiation and germ cell pool maintenance“. I wrote this thesis independently and without assistance from third parties, I used no other aids than the listed sources and resources.

All points based literally or in spirit on publications or presentations of other authors are, as such, in proper citations (see "uniform requirements for manuscripts (URM)" the ICMJE www.icmje.org) indicated. The sections on methodology (in particular practical work, laboratory requirements, statistical processing) and results (in particular images, graphics and tables) correspond to the URM (s.o) and are answered by me. My contributions in the selected publications for this dissertation correspond to those that are specified in the following joint declaration with the responsible person and supervisor. All publications resulting from this thesis and which I am author of correspond to the URM (see above) and I am solely responsible.

The importance of this affidavit and the criminal consequences of a false affidavit (section 156,161 of the Criminal Code) are known to me and I understand the rights and responsibilities stated therein.

Date

Signature

8. Declaration of any eventual publications

Sami Zaqout had the following share in the following publications:

Publication 1:

Nadine Kraemer, Ethiraj Ravindran, **Sami Zaqout**, Gerda Neubert, Detlev Schindler, Olaf Ninnemann, Ralph Gräf, Andrea EM Seiler, Angela M Kaindl. Loss of CDK5RAP2 affects neural but not nonneural mESC differentiation into cardiomyocytes. *Cell Cycle* 2015; 14:2044-57. (Impact factor 2015 = 3.952)

Contribution in detail: Sami Zaqout performed the apoptosis analysis for neurally differentiating mESC and proofread the manuscript.

Publication 2:

Sami Zaqout, Angela M Kaindl. Golgi-Cox staining step by step. *Frontiers in Neuroanatomy* 2016; 10:38-45. (Impact factor 2015 = 3.260)

Contribution in detail: Sami Zaqout describe the Golgi-Cox staining in such detail that should turn the staining into an easily feasible method for all scientists working in the neuroscience field. He isolated murine brain samples, prepared all related chemical solutions, cut and stained the brain sections. He also created figures, interpreted the data, drafted and revised the manuscript.

Publication 3:

Sami Zaqout, Paraskevi Bessa, Nadine Krämer, Gisela Stoltenburg-Didinger, Angela M Kaindl. CDK5RAP2 is required to maintain the germ cell pool during embryonic development. *Stem Cell Reports* 2017; in press. (Impact factor 2015 = 7.023)

Contribution in detail: Sami Zaqout isolated murine testicular and embryonic samples, prepared paraffin section, applied H&E and immunostaining for several germ cell-related markers. He helped with the injection of Iddu/Brdu substances and performed all analysis for germ cell. He also interpreted the data, created figures, drafted and revised the manuscript.

Signature, date and stamp of the supervising University teacher

Signature of the doctoral candidate

8.1 Loss of CDK5RAP2 affects neural mESC differentiation

Kraemer N, Ravindran E, **Zaqout S**, Neubert G, Schindler D, Ninnemann O, Graf R, Seiler AE, Kaindl AM. Loss of CDK5RAP2 affects neural but not non-neural mESC differentiation into cardiomyocytes. *Cell Cycle* 2015; 14:2044-57

Biallelic mutations in the gene encoding centrosomal CDK5RAP2 lead to autosomal recessive primary microcephaly (MCPH), a disorder characterized by pronounced reduction in volume of otherwise architectonically normal brains and intellectual deficit. The current model for the microcephaly phenotype in MCPH invokes a premature shift from symmetric to asymmetric neural progenitor-cell divisions with a subsequent depletion of the progenitor pool. The isolated neural phenotype, despite the ubiquitous expression of CDK5RAP2, and reports of progressive microcephaly in individual MCPH cases prompted us to investigate neural and non-neural differentiation of Cdk5rap2-depleted and control murine embryonic stem cells (mESC). We demonstrate an accumulating proliferation defect of neurally differentiating Cdk5rap2-depleted mESC and cell death of proliferative and early postmitotic cells. A similar effect does not occur in non-neural differentiation into beating cardiomyocytes, which is in line with the lack of non-central nervous system features in MCPH patients. Our data suggest that MCPH is not only caused by premature differentiation of progenitors, but also by reduced propagation and survival of neural progenitors.

<http://dx.doi.org/10.1080/15384101.2015.1044169>



Golgi-Cox Staining Step by Step

Sami Zaqout^{1,2*} and Angela M. Kaindl^{1,2}

¹ Institute of Cell Biology and Neurobiology, Charité – Universitätsmedizin Berlin, Berlin, Germany, ² Center for Chronically Sick Children (Sozialpädiatrisches Zentrum, SPZ), Charité – Universitätsmedizin Berlin, Berlin, Germany

Golgi staining remains a key method to study neuronal morphology *in vivo*. Since most protocols delineating modifications of the original staining method lack details on critical steps, establishing this method in a laboratory can be time-consuming and frustrating. Here, we describe the Golgi-Cox staining in such detail that should turn the staining into an easily feasible method for all scientists working in the neuroscience field.

Keywords: Golgi, neuronal morphology, spines, dendrites, vibratome

INTRODUCTION

Studying neuronal morphology is more relevant than ever given the rapid identification of novel genetic neurodevelopmental diseases through next-generation sequencing approaches and the subsequent need to understand underlying pathomechanisms. Discovered already by Golgi (1873), the non-invasive Golgi staining method is far from out-of-date, and it facilitates an analysis of neuronal morphology with axonal and dendritic arborization and spines through visualization of only a low percentage of neurons (1–3%). Three major Golgi staining subtypes exist: Rapid Golgi, Golgi-Kopsch, and Golgi-Cox (Koyama, 2013). Of these, the Golgi-Cox method is considered to be most reliable in demonstrating dendritic arborization with a low background (Buell, 1982; Koyama, 2013). Many modifications of this method have been conducted and most aimed to increase its reliability (Angulo et al., 1996; Gibb and Kolb, 1998; Koyama and Tohyama, 2012), to reduce the required time (Ranjan and Mallick, 2010; Levine et al., 2013; Patro et al., 2013), and to increase the selectivity of neuronal vs. glial staining or *vice versa* (Ranjan and Mallick, 2012; Gull et al., 2015). Also, commercial kits have been developed for relatively fast constant Golgi staining. However, most Golgi staining descriptions lack exact details of individual steps. Here, we report in detail all steps of the Golgi-Cox staining method on adult mouse brain vibratome sections required for a reliable high quality staining in an acceptable time frame and with well-preserved tissue quality. The materials applied are available in most neuroscience labs and sufficient to establish the Golgi-Cox staining for many samples. Following our protocol step-by-step will likely minimize troubles encountered frequently and reduce the time required to standardize this method.

OPEN ACCESS

Edited by:

Francesco Fornai,
University of Pisa, Italy

Reviewed by:

Luis Puelles,
Universidad de Murcia, Spain
Tom Reese,
National Institutes of Health, USA

***Correspondence:**

Sami Zaqout
sami.zaqout@charite.de

Received: 09 December 2015

Accepted: 21 March 2016

Published: 31 March 2016

Citation:

Zaqout S and Kaindl AM (2016)
Golgi-Cox Staining Step by Step.
Front. Neuroanat. 10:38.
doi: 10.3389/fnana.2016.00038

MATERIALS, EQUIPMENT AND STEPWISE PROCEDURES

Mice

Adult 6–12-week-old C57BL/6 mice were obtained from the animal facility of the Charité—Universitätsmedizin Berlin, Germany. All experiments were carried out in accordance to the national ethic principles (registration no. T0309.09).

General Instructions Before Starting

1. All glass and plastic bottles should be rinsed with fresh double distilled water (dd-H₂O) before use.
2. Plastic-coated magnetic stirring pills (rods) can be used to dissolve all chemicals in dd-H₂O properly.
3. Metal instruments must be avoided during the impregnation step.
4. The amount of solutions and gelatin-coated slides should be prepared according to the number of samples as indicated in each section.
5. The incubation time frame given for various steps in this protocol are periods that do not affect significantly the staining quality. Thus, these time frames provide some flexibility when pursuing with the protocol.
6. All solutions must be stored in the dark using aluminum foil to cover large bottles, or by placing small bottles in a covered, lightproof box.
7. Care should be taken with all solutions due to toxicity and carcinogenesis: direct skin contact and inhalation can be avoided by wearing gloves and performing the experiments under a chemical hood, respectively.

Preparation of Solutions

Solution for Sample Impregnation

The impregnation stock solutions are prepared by dissolving 15 g from of the following chemicals in 300 ml dd-H₂O (5% w/v) each:

1. Potassium dichromate (K₂Cr₂O₇; 1.04862, Merck KGaA, Germany).
2. Mercuric chloride (HgCl₂; KK04.2, Carl Roth GmbH, Germany).
3. Potassium chromate (K₂CrO₄; HN33.2, Carl Roth GmbH, Germany).

All three solutions, stored in bottles at room temperature in the dark, are for long-term usage to prepare Golgi-Cox solution. These solutions are sufficient for 36 adult mouse brains. Golgi-Cox solution is prepared for each experiment in a new bottle using the three stock solutions mentioned above as follows (Rutledge et al., 1969).

1. 50 ml of the potassium dichromate solution is mixed with 50 ml of the mercuric chloride solution.
2. 40 ml of the potassium chromate solution is added.
3. 100 ml of dd-H₂O is added.

After mixing the solution, the bottle needs to be covered with aluminum foil and kept to settle at room temperature for at least 48 h before use to allow precipitate formation. This solution is sufficient for six adult mouse brains and can be used for up to 1 month.

Solution for Tissue Protection

First, 0.1 M phosphate buffer (pH 7.2) is prepared by dissolving the following components together in 500 ml dd-H₂O:

1. 1.59 g sodium-hydrogen-phosphate monohydrate (NaH₂PO₄·H₂O; T878.3, Carl Roth GmbH, Germany).

2. 5.47 g di-sodium-hydrogen-phosphate water-free (Na₂HP0₄; P030.2, Carl Roth GmbH, Germany).
3. 9.0 g sodium chloride (NaCl; 9265.1, Carl Roth GmbH, Germany).

Second, 1000 ml of a tissue-protectant (cryoprotectant) solution (de Olmos et al., 1978; Watson et al., 1986) is prepared by dissolving the following components in the previous 500 ml phosphate buffer:

1. 300 g sucrose (C₁₂H₂₂O₁₁; 1.07687, Merck KGaA, Germany).
2. 10 g polyvinylpyrrolidone (PVP40, Sigma-Aldrich, Germany).
3. 300 ml ethylene glycol (C₂H₆O₂; E-9129, Sigma-Aldrich, Germany).

The final volume is then adjusted to 1000 ml with dd-H₂O. 500 ml of the solution can be kept in a separate bottle to fill the vibratome chamber and the rest is sufficient to pursue with the tissue protection step for 25 adult mouse brains. This solution needs to be stored at 4°C in the dark for long term storage.

Solutions for the Developing Step

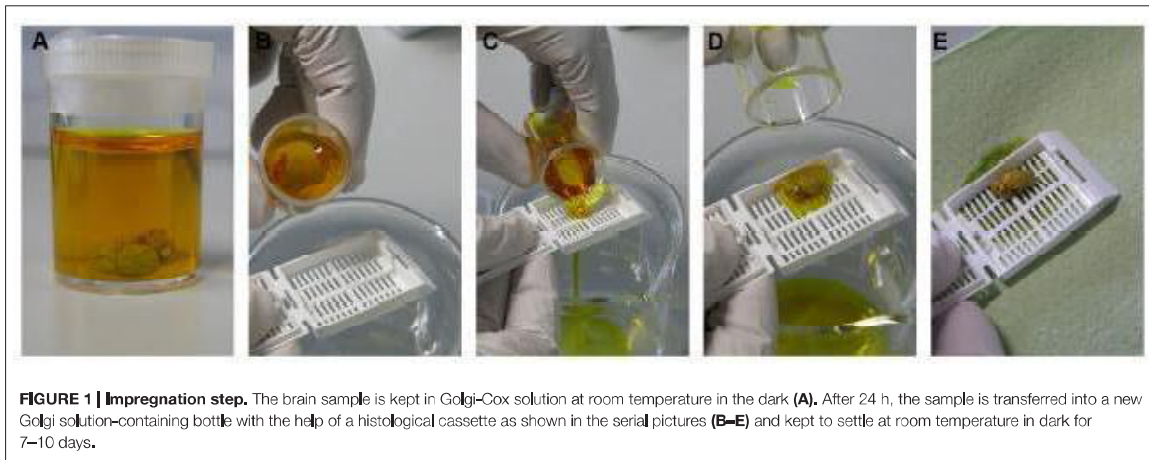
For the developing step, about 300 ml from each of the following solutions are needed:

1. 50, 70, 95, and 100% ethanol series (C₂H₆O; K928.4, Carl Roth GmbH, Germany).
2. Xylene (C₈H₁₀; 9713.3, Carl Roth GmbH, Germany).
3. 3:1 ammonia:dd-H₂O is prepared by mixing 200 ml ammonia (NH₃·H₂O; 6774.2, Carl Roth GmbH, Germany) with 100 ml dd-H₂O.
4. 5% sodium thiosulfate is prepared by dissolving 15 g sodium thiosulfate (Na₂S₂O₃·5H₂O; 2781895, Merck KGaA, Germany) in 300 ml dd-H₂O.

All solutions are stored at room temperature and the bottle with the sodium thiosulfate solution is covered with aluminum foil. These solutions can be re-used and should be replaced when they turn dark.

Solutions and Materials for Gelatin-Coated Slides

Seventy five plain microscopic slides (micro slides; 2406/1, Glaswarenfabrik Karl Hecht GmbH and Co KG) are first placed in three staining racks (2285.1, Carl Roth GmbH, Germany), washed thoroughly with dd-H₂O and kept for drying in a dust-free area (e.g., under a chemical hood) for 2–3 h. In the meantime, 3% gelatin is prepared by dissolving 9 g gelatin from porcine skin (Type A; G2500, Sigma-Aldrich, Germany) in 300 ml dd-H₂O with constant stirring and heating to 55°C. The solution is then filtered with filter paper (240 mm; 4.303.240, Neolab, Germany) into a clean histological staining box (2285.1, Carl Roth GmbH, Germany). A rack with the cleaned slides is immersed into the warm gelatin solution for 10 min, subsequently placed on plenty tissue papers and kept at room temperature in a dust-free area overnight. The gelatin should be re-warmed to 55°C before immersing a further rack of slides. These slides are sufficient for 200 μm thick-brain sections collected



from six adult mouse brains. If more than three racks are needed, more 3% gelatin solution needs to be prepared. These gelatin-coated slides need to be stored in closed histological staining boxes and are best to be used within a month of preparation.

Impregnation Step

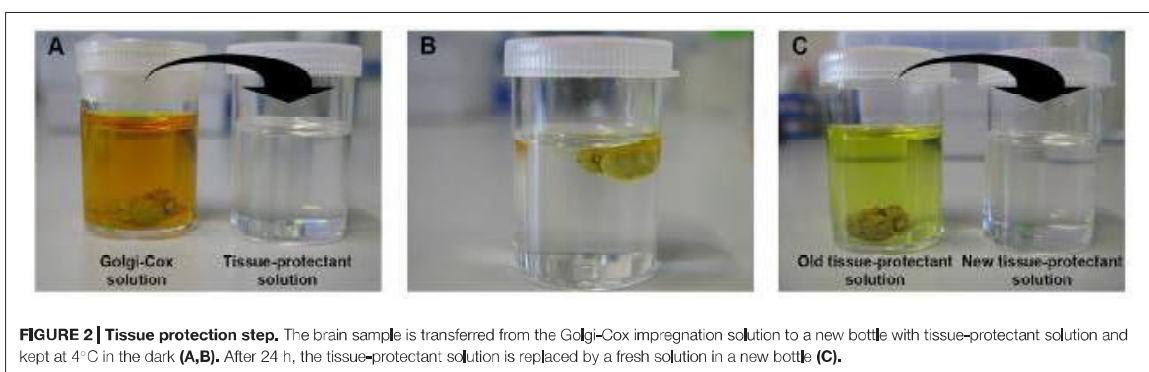
For each brain sample, one small bottle (multi-purpose container with lid; 203170, Greiner bio-one, Germany) is washed with dd-H₂O. The aluminum foils are removed gently from the Golgi-Cox bottle without shaking, to avoid the solution mixing with brownish precipitates at the bottom of the bottle. For each sample, 10 ml is taken from the upper clear part of Golgi-Cox solution and dispensed into each small bottle.

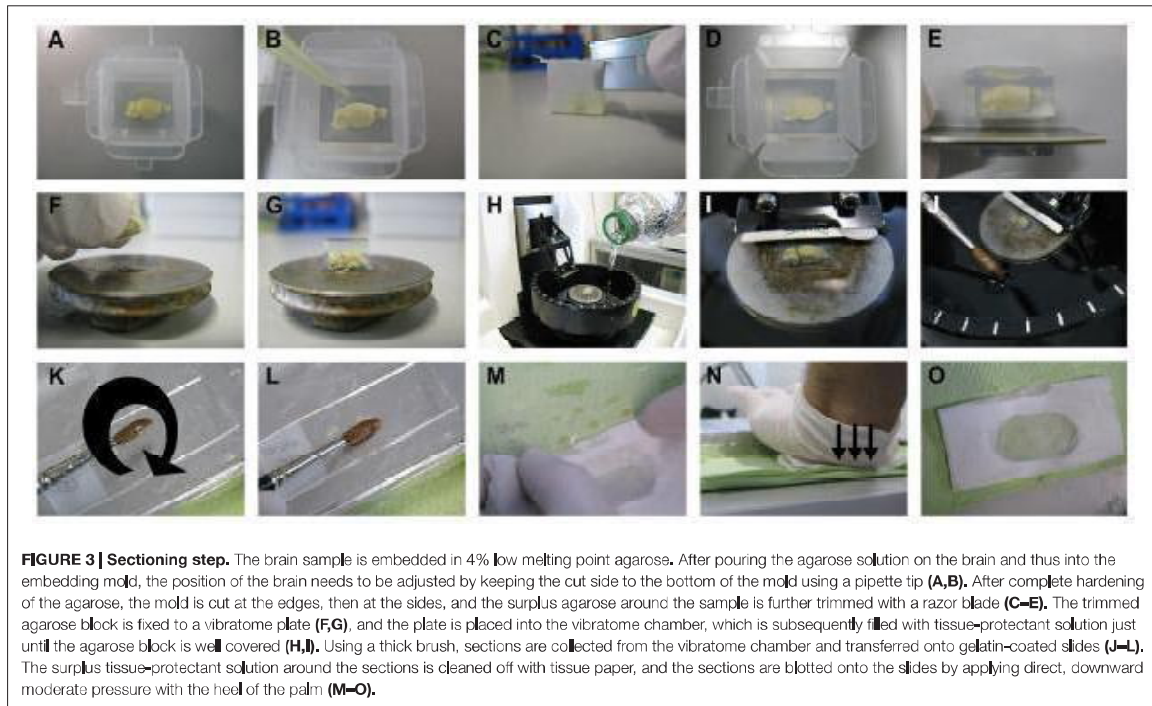
After cervical dislocation, the brain is dissected quickly but carefully, washed with dd-H₂O, and cut into two halves to allow better impregnation. Each half is then transferred into an individual small bottle with Golgi-Cox solution (Figure 1A) and stored at room temperature in dark. Fixation or perfusion

with 4% PFA of adult brains should be avoided because this leads to over-impregnated neurons rendering a study of neuronal arborization impossible. After 24 h, each brain sample is transferred into a new small bottle of Golgi-Cox solution using plastic forceps or preferably by pouring the solution and sample into histological cassettes (Rotilabo[®] embedding cassettes; K114.1, Carl Roth GmbH, Germany) as shown in Figures 1B–E. The small bottles are kept at room temperature in the dark for 7–10 days.

Tissue Protection Step

For each brain sample, one small bottle, as described above, is washed with dd-H₂O and filled with 10 ml tissue-protectant solution. With the help of histological cassettes, as described above, each brain sample is transferred from Golgi-Cox solution to tissue-protectant solution (Figures 2A,B), and stored at 4°C in dark. After 24 h, each brain sample is transferred into a new small bottle with 10 ml tissue-protectant solution (Figure 2C). The small bottles are kept at 4°C in dark for 4–7 days.

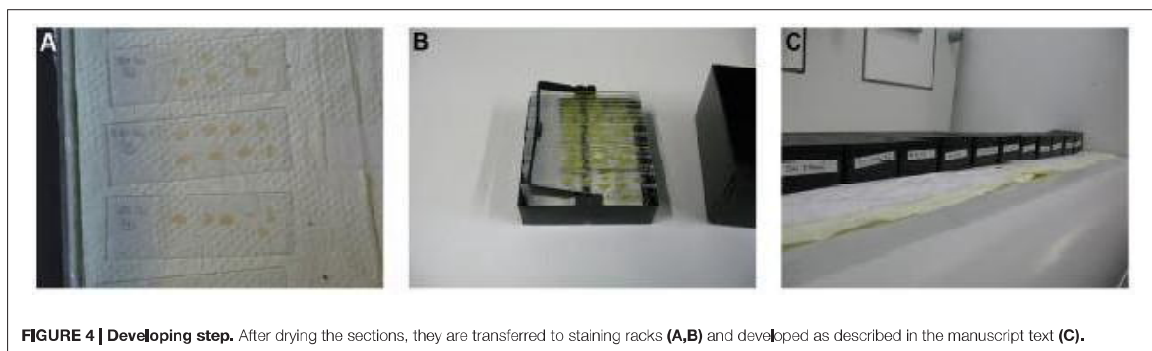


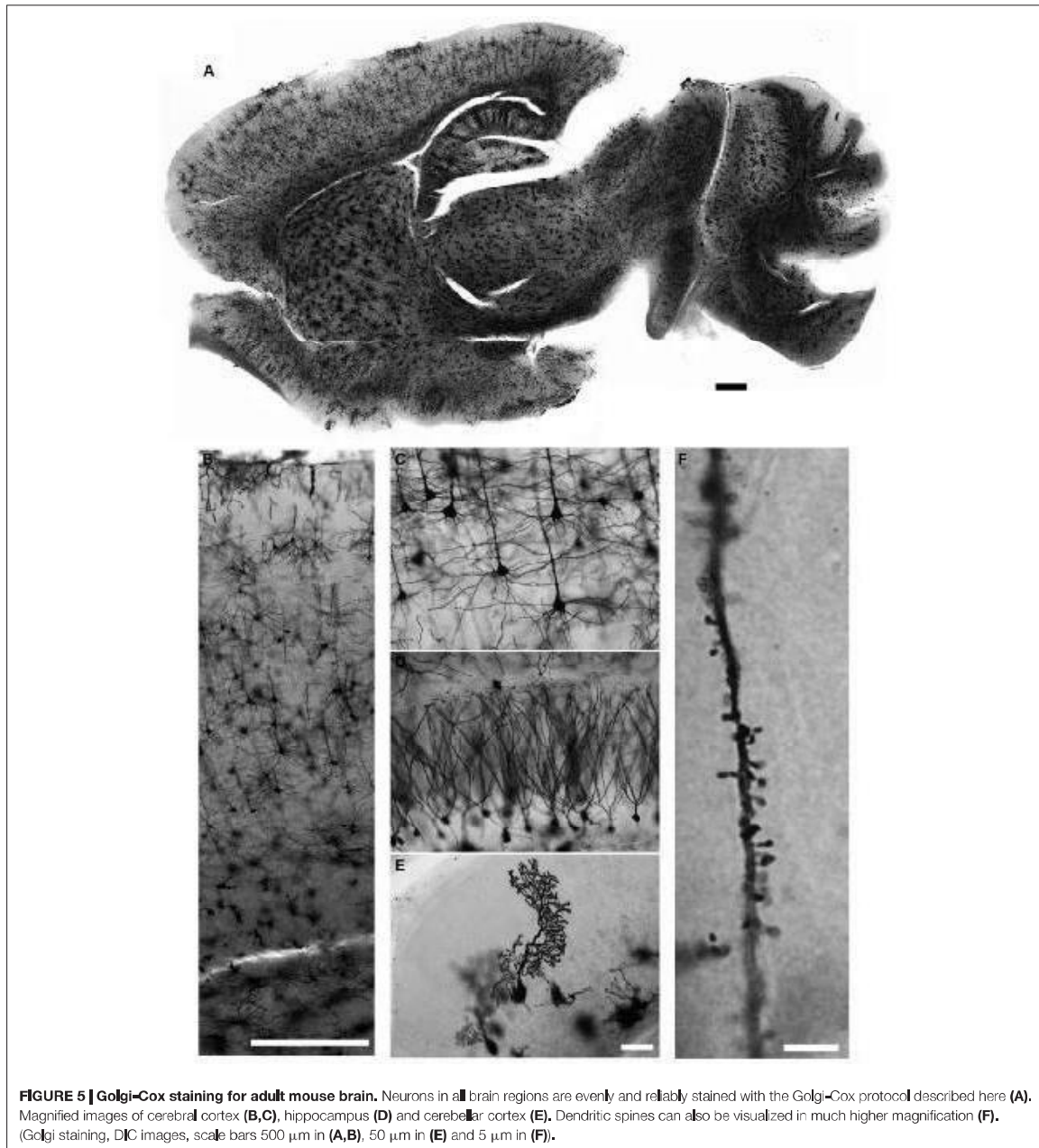


Sectioning Step

For our procedure, vibratome (Microm; HM_650V, Thermo Fisher Scientific Inc., Germany) was used for tissue sectioning as described below and shown in Figure 3. Cryostat or sliding-freezing microtome should also work fine as fully described in the protocol of the commercially available FD Rapid GolgiStain™ Kit (FD Neurotechnologies, Inc., MD, USA). For sectioning using a vibratome, 4% agarose is prepared by dissolving 2 g low melting point agarose (V2111, Promegain, WI, USA) in 50 ml dd-H₂O by stirring first and then using a microwave until completely dissolved. Brain samples are then gently dried on tissue paper with the help of histological

cassettes, as described above, and transferred into disposable plastic embedding molds (18646A, Polysciences Inc., PA, USA; Figure 3A). When the agarose temperature has cooled down to 47°C, it is poured into the molds until the brain samples are well covered with solution. The orientation of the brain needs to be adjusted with a pipette tip by keeping the medial cut side of the brain at the bottom of the mold (Figure 3B). If the most medial part of the brain sample is needed for sectioning, a thin layer of agarose should be poured into the bottom of the mold, and the mold should then be kept at 4°C for hardening. The brain sample can be then transferred as described above. After complete hardening of





agarose, the edges of the molds are cut using a razor blade and surplus agarose around the brain sample is trimmed (Figures 3C–E).

With one drop of fast glue (Instant adhesive; E10C589, Best-CA, Germany), the brain sample is fixed to the vibratome plate (Figures 3F,G), and the plate is placed in the vibratome

chamber. Subsequently, the vibratome chamber is filled with tissue-protectant solution and the cutting razor blade (Sward Classic, 7000115z, Wilkinson GmbH, Germany) put in place (Figures 3H,I). In our hands, a vibration frequency of 60 Hz and a speed to 15 mm/s works best, but these values can be changed according to the quality of cutting. The section thickness

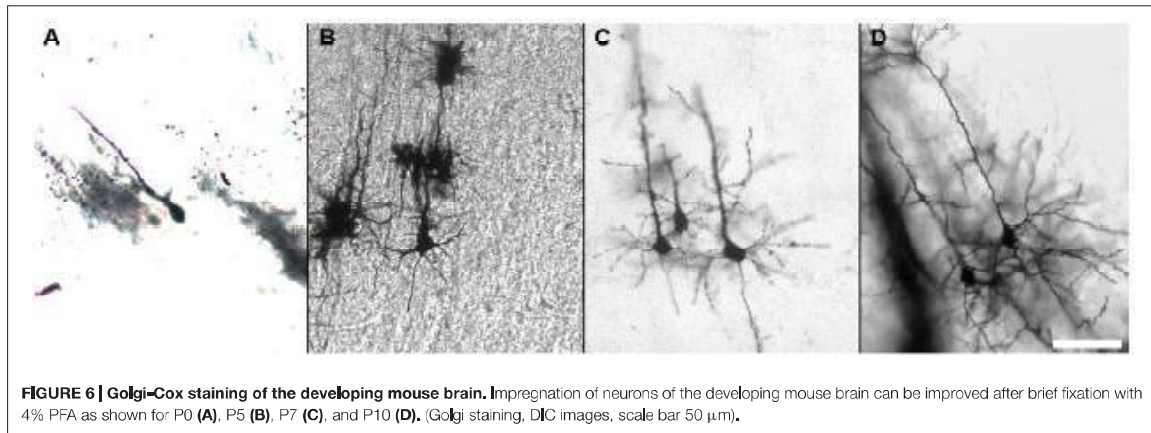


FIGURE 6 | Golgi-Cox staining of the developing mouse brain. Impregnation of neurons of the developing mouse brain can be improved after brief fixation with 4% PFA as shown for P0 (A), P5 (B), P7 (C), and P10 (D). (Golgi staining, DIC images, scale bar 50 μm).

is optimally 200 μm for dendritic arborization studies and 100 μm for dendritic spines studies. While cutting, sections are collected with a thick brush and transferred onto gelatin-coated slides (Figures 3J–L). As soon as all sections have been loaded on slides, the surplus tissue-protectant solution around the sections is cleaned off with absorbent paper (Figure 3M). The sections are then blotted by pressing an absorbent paper moistened with tissue-protectant solution onto the slides. The best way, as described previously, is by applying direct, downward moderate pressure with the heel of the palm (Gibb and Kolb, 1998; Figures 3N,O). If the sections stick to the absorbent paper, then the paper is likely not soaked sufficiently with tissue-protectant solution. The slides with sections are transferred to racks and kept for drying in dark for 2–3 days.

After finishing the sectioning of all samples, the tissue-protectant solution in the vibratome chamber can be filtered with filter paper (240 mm; 4.303.240, Neolab, Germany) into a bottle, kept at 4°C in dark and re-used several times. However, this filtered tissue-protectant solution should be used only to fill the vibratome chamber and not for the tissue protection step.

Developing Step

Using common histological staining boxes, the racks with slides are dehydrated and developed as follows (Figure 4):

1. Distilled water twice for 5 min each.
2. 50% ethanol for 5 min.
3. 3:1 ammonia solution for 8 min.
4. Distilled water twice for 5 min each.
5. 5% sodium thiosulfate for 10 min in dark.
6. Distilled water twice for 1 min each.
7. Optionally, sections can be incubated in 1% cresyl violet (as a counterstain) for 5 min.
8. 70, 95, and 100% ethanol for 6 min each.
9. Xylol for 6 min, and the sections can be kept in xylol longer until the mounting step.

We found that these steps are sufficient to receive good results; however the last two steps (dehydration with ethanol and cleaning with xylol) can be duplicated for further quality improvement.

Mounting Step

For mounting, only two slides are taken from the xylol box per step and kept for about 1 min until they are semidry. Depending on the thickness of the sections, 5 (for 100 μm thick-sections) to 10 (for 200 μm thick-sections) drops of Fukitt (quick-hardening mounting medium; 03989, Fluka Analytical, Germany) are added. The slides are then covered with cover glass and air bubbles avoided by applying light pressure. After finishing the mounting of all samples, the slides are sealed with nail polish. The slides are then kept in a horizontal position for drying in the dark for 48 h before imaging. The sections can be subsequently stored in slide boxes in the dark at room temperature for long time usage.

Imaging

In our laboratory, 1- μm -spaced Z-stack brightfield images for dendritic arborization studies are optimal in our hands and are taken by an Olympus IX81 microscope equipped with a F View II (sw) camera (Soft Imaging System GmbH, Münster, Germany). Brightfield images for dendritic spines are taken by Olympus BX60 microscope with AxioCam MRc Zeiss camera and Axiovision 4.8 Software (Zeiss, Göttingen, Germany). All images are processed using Adobe Photoshop CS6 version 13.0 \times 64 and ImageJ Software. The magnification and quality of the spine images can be increased using Transform J Scale plug-in available for the ImageJ Software.

RESULTS AND DISCUSSION

We describe in detail the Golgi-Cox staining protocol from preparation of the solutions, via transferring brain tissue, tissue sectioning, and development to mounting of the stained sections.

Using this protocol, we have found that the dendritic tree and the dendritic spines of neurons are evenly and constantly stained in all brain regions (Figure 5). Additionally, while most Golgi-based studies report using coronal sections, we have found that neuronal dendritic arborization is best preserved and imaged when brains are cut in the sagittal plane, as also note by Valverde (1998). We also found that the tissue-protectant (cryoprotectant) solution (de Olmos et al., 1978; Watson et al., 1986) is very helpful to preserve tissue quality, reduce the staining background, and improve the attachment of sections to gelatin-coated slides. Minor additional steps can be added to our protocol to amend it for younger mice (Koyama and Tohyama, 2012) or to increase the staining for glia cells more than neurons (Ranjan and Mallick, 2012; Gull et al., 2015). Using our protocol, we found that initial brief fixation of brain samples with 4% PFA for 1 h followed by dd-H₂O washing improves the staining for younger mice (Figure 6). Once all chemical and materials available in the lab, Golgi staining can be performed for large number of brain samples that lowers the overall cost needed to perform this staining.

REFERENCES

- Angulo, A., Fernandez, E., Merchan, J. A., and Molina, M. (1996). A reliable method for Golgi staining of retina and brain slices. *J. Neurosci. Methods* 66, 55–59. doi: 10.1016/0165-0270(95)00160-3
- Buell, S. J. (1982). Golgi-Cox and rapid Golgi methods as applied to autopsied human brain tissue: widely disparate results. *J. Neuropathol. Exp. Neurol.* 41, 500–507. doi: 10.1097/00005072-198209000-00003
- de Olmos, J., Hardy, H., and Heimer, L. (1978). The afferent connections of the main and the accessory olfactory bulb formations in the rat: an experimental HRP-study. *J. Comp. Neurol.* 81, 213–244. doi: 10.1002/cne.901810202
- Gibb, R., and Kolb, B. (1998). A method for vibratome sectioning of Golgi-Cox stained whole rat brain. *J. Neurosci. Methods* 79, 1–4. doi: 10.1016/s0165-0270(97)00163-5
- Golgi, C. (1873). Sulla struttura della sostanza grigia della cervello. *Gazz. Med. Ital. Lombardia.* 6, 244–246.
- Gull, S., Ingrisch, I., Tausch, S., Witte, O. W., and Schmidt, S. (2015). Consistent and reproducible staining of glia by a modified Golgi-Cox method. *J. Neurosci. Methods* 256, 141–150. doi: 10.1016/j.jneumeth.2015.08.029
- Koyama, Y. (2013). The unending fascination with the Golgi method. *OA Anatomy* 1:24. doi: 10.13172/2052-7829-1-3-848
- Koyama, Y., and Tohyama, M. (2012). A modified and highly sensitive Golgi-Cox method to enable complete and stable impregnation of embryonic neurons. *J. Neurosci. Methods* 209, 58–61. doi: 10.1016/j.jneumeth.2012.06.007
- Levine, N. D., Rademacher, D. J., Collier, T. J., O'Malley, J. A., Kells, A. P., San Sebastian, W., et al. (2013). Advances in thin tissue Golgi-Cox impregnation: fast, reliable methods for multi-assay analyses in rodent and non-human primate brain. *J. Neurosci. Methods* 213, 214–227. doi: 10.1016/j.jneumeth.2012.12.001
- Patro, N., Kumar, K., and Patro, I. (2013). Quick Golgi method: modified for high clarity and better neuronal anatomy. *Indian J. Exp. Biol.* 51, 685–693. doi: 10.13172/2052-7829-1-3-848
- Ranjan, A., and Mallick, B. N. (2010). A modified method for consistent and reliable Golgi-cox staining in significantly reduced time. *Front. Neurol.* 1:157. doi: 10.3389/fneur.2010.00157
- Ranjan, A., and Mallick, B. N. (2012). Differential staining of glia and neurons by modified Golgi-Cox method. *J. Neurosci. Methods* 209, 269–279. doi: 10.1016/j.jneumeth.2012.06.023
- Rutledge, L. T., Duncan, J., and Beatty, N. (1969). A study of pyramidal cell axon collaterals in intact and partially isolated adult cerebral cortex. *Brain Res.* 16, 15–22. doi: 10.1016/0006-8993(69)90082-1
- Valverde, F. (1998). *Golgi Atlas of the Postnatal Mouse Brain*, (Vienna: Springer).
- Watson, R. E., Wiegand, S. J., Clough, R. W., and Hoffman, G. E. (1986). Use of cryoprotectant to maintain long-term peptide immunoreactivity and tissue morphology. *Peptides* 7, 155–159. doi: 10.1016/0196-9781(86)90076-8

CONCLUSION

Applying this protocol renders Golgi staining easily feasible for all laboratories working on neuroscience projects.

AUTHOR CONTRIBUTIONS

SZ performed the experiments. SZ and AMK were responsible for the project conception and wrote as well as approved the final manuscript.

ACKNOWLEDGMENTS

This work was supported by the German Research Foundation (DFG, SFB665), the Helmholtz Association by the Berlin Institute of Health (BIH), the German Academic Exchange Service (DAAD), and the Charité – Universitätsmedizin Berlin. We thank Jutta Schüler for our institute for microscopy advice and Emma Perez-Costas (Department of Psychology and Department of Pediatrics; University of Alabama at Birmingham) for technical advice.

Conflict of Interest Statement: The authors declare that the research was conducted in the absence of any commercial or financial relationships that could be construed as a potential conflict of interest.

Copyright © 2016 Zaqout and Kaindl. This is an open-access article distributed under the terms of the Creative Commons Attribution License (CC BY). The use, distribution and reproduction in other forums is permitted, provided the original author(s) or licensor are credited and that the original publication in this journal is cited, in accordance with accepted academic practice. No use, distribution or reproduction is permitted which does not comply with these terms.

8.3 Germ cell depletion in an/an

Please cite this article in press as: Zaqout et al., CDK5RAP2 Is Required to Maintain the Germ Cell Pool during Embryonic Development, Stem Cell Reports (2017), <http://dx.doi.org/10.1016/j.stemcr.2017.01.002>

Stem Cell Reports

Report



OPEN ACCESS

CDK5RAP2 Is Required to Maintain the Germ Cell Pool during Embryonic Development

Sami Zaqout,^{1,2,3} Paraskevi Bessa,¹ Nadine Krämer,^{1,2,3} Gisela Stoltenburg-Didinger,¹ and Angela M. Kaindl^{1,2,3,*}

¹Institute of Cell Biology and Neurobiology, Charité – Universitätsmedizin Berlin, Charitéplatz 1, 10117 Berlin, Germany

²Center for Chronically Sick Children (Sozialpädiatrisches Zentrum, SPZ), Charité – Universitätsmedizin Berlin, Augustenburger Platz 1, 13353 Berlin, Germany

³Berlin Institute of Health (BIH), Kapelle-Ufer 2, 10117 Berlin, Germany

*Correspondence: angela.kaindl@charite.de

<http://dx.doi.org/10.1016/j.stemcr.2017.01.002>

SUMMARY

Gene products linked to microcephaly have been studied foremost for their role in brain development, while their function in the development of other organs has been largely neglected. Here, we report the critical role of *Cdk5rap2* in maintaining the germ cell pool during embryonic development. We highlight that infertility in *Cdk5rap2* mutant mice is secondary to a lack of spermatogenic cells in adult mice as a result of an early developmental defect in the germ cells through mitotic delay, prolonged cell cycle, and apoptosis.

INTRODUCTION

Biallelic mutations in the cyclin-dependent kinase-5 regulatory subunit-associated protein 2 gene *CDK5RAP2* cause autosomal recessive primary microcephaly type 3 (MCPH3), a rare disease characterized by severe congenital microcephaly and intellectual disability (Bond et al., 2005; Kaindl et al., 2010; Kraemer et al., 2011; Moynihan et al., 2000). MCPH is acknowledged as a model disorder for an isolated brain phenotype. Recent data link the brain phenotype to a stem cell defect with premature shift from symmetric to asymmetric progenitor cell divisions, leading to premature neurogenesis, a depletion of the progenitor pool, and a reduction of the final number of neurons (Buchman et al., 2010; Fish et al., 2006; Kaindl et al., 2010; Lizarraga et al., 2010). In addition, reduced propagation and survival of differentiating neural progenitors have been shown (Kraemer et al., 2015).

Despite the highlighted brain phenotype, it needs to be noted that *Cdk5rap2* is ubiquitously expressed (Issa et al., 2013) and exerts functions such as maintaining centrosome function, spindle assembly and orientation, and/or cell cycle checkpoint control (Kraemer et al., 2011; Megraw et al., 2011) that are likely relevant also to other organs. So far, no progeny of affected humans has been reported, indicating a potential role of CDK5RAP2 for the germline. Moreover, a loss of the *CDK5RAP2* homologous gene centrosomin (*cmn*) in *Drosophila* causes malfunctions in meiotic centrosomes and spermatid basal bodies leading to male sterility (Li et al., 1998). *Cdk5rap2* mutant or Hertwig's anemia (*an/an*) mice were known solely for their hematopoietic phenotype (macrocytic, hypoproliferative anemia, leukopenia) prior to their identification as an MCPH3 model with microcephaly in 2010 (Lizarraga

et al., 2010). Homozygous male *Cdk5rap2* mutant mice are infertile secondary to a severe germ cell deficiency, and females cannot deliver pups (Lizarraga et al., 2010; Russell et al., 1985). Here, we show that germ cell depletion in *an/an* mice occurs already during early development through a mitotic delay, prolonged cell cycle, and apoptosis.

RESULTS AND DISCUSSION

Hypomorphic Gross Phenotype and Embryonic Lethality

The *an/an* mice can be recognized by their characteristic hypomorphic gross phenotype apparent at birth (Figures 1A and 1A'). While the expected Mendelian ratio of *an/an* mice was found at embryonic days E12.5–E14.5 (*an/an*: *an/+*: *+/+* = 24: 43: 16), only 9.5% of the offspring carried a homozygous mutant genotype (*an/an*) at P0 (*an/an*: *an/+*: *+/+* = 46: 287: 152; Figure S1), indicating in utero lethality.

Sterility in Male Mice

Testes of *an/an* mice at both P0 and adult ages were severely reduced in cross-sectional area, weight, and testes/body weight ratio (Figures 1B–1F'). Further analysis of H&E-stained testes revealed the absence of gonocytes in P0 *an/an* testes and of all spermatogenic cells from spermatogonia to mature sperms in adult *an/an* testes (Figures 1G and 1G'). We further confirmed this by immunostaining, applying germ cell markers anti-mouse vasa homolog (MVH) and anti-germ cell-specific antigen (TRA98) (Figure 2A and data not shown). The seminiferous tubules, demarcated by Sertoli cells, were normal in architecture, but notably

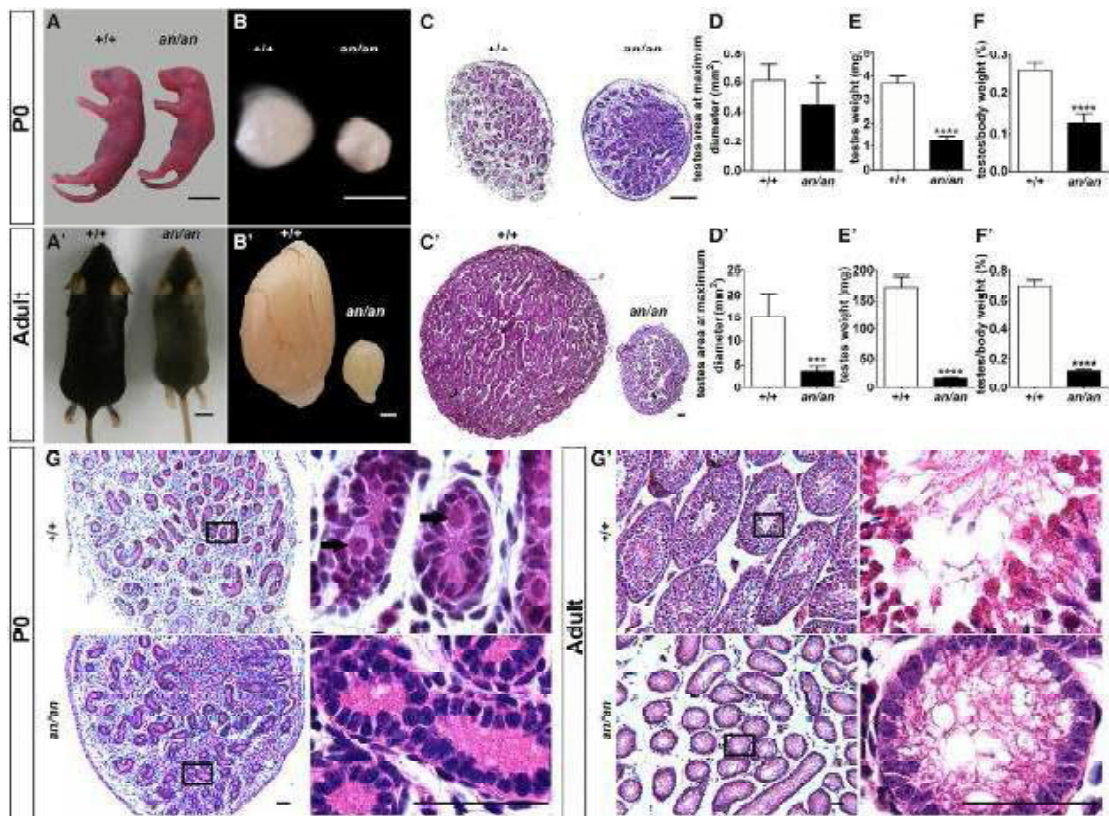


Figure 1. Testes of *Cdk5rap2* Mutant Mice Lack Germ Cells

(A–B') Hypomorphic gross phenotype and reduced testis size of P0 and adult *an/an* mice. Scale bars, 10 mm (A and A') and 1 mm (B and B'). (C–D') Testis area is reduced in P0 and adult *an/an* mice at the position of maximal testis diameter. Scale bars, 200 μ m, n = 6–7 animals/group.

(E–F') Reduction of testis weight and testis/body weight is already present at P0 in *an/an* mice and also significant in adult mice. n = 3–6 (P0) and n = 6–7 (adult) animals/group.

(G–G') Absence of gonocytes (arrows) in seminiferous tubules at P0 and of spermatogenic cells in adult *an/an* mice. Scale bars, 50 μ m, H&E staining, differential interference contrast images.

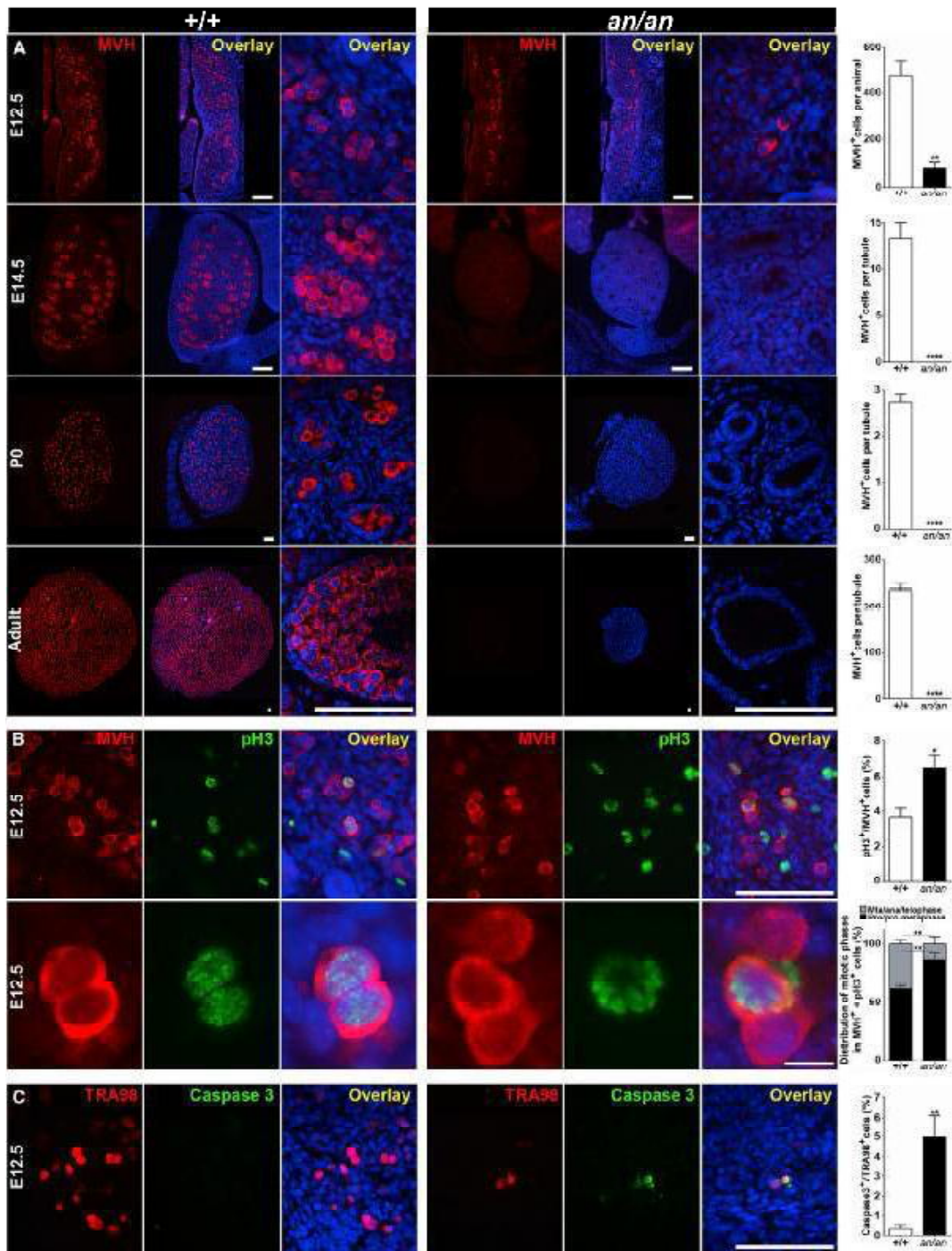
Error bars indicate SD, Student's t test, *p < 0.05, ***p < 0.001, ****p < 0.0001.

smaller in size in *an/an* mice due to lack of the germ cells. The Sertoli and Leydig cells appear normal, suggesting that these testicular somatic cells play no major role in *an/an* germ cell phenotype. Intriguingly, neither uterus nor ovaries could be detected in adult *an/an* females (Figure S2).

Lack of Germ Cells in *an/an* Mice Is due to an Early Developmental Defect

The absence of germ cells in *an/an* males at P0 points toward an earlier developmental defect in the germline. Normally, germ cells in mice are specified at E6.25–7.25, proliferate

and migrate toward the genital ridge at E8.5–12.5, and undergo mitotic arrest at E12.5–E14.5 in males (De Felici, 2009; McLaren, 2003; Western et al., 2008). The current availability of germ cell markers and the advantage of immunohistochemistry techniques allowed us to explore the exact time period when these cells are lost in *an/an* mice during development. For this, we studied embryonic sections of *an/an* mice at the level of the testes and the genital ridges at E14.5 and E12.5, respectively. At E14.5, testes of *an/an* mice lacked gonocytes positive for MVH or TRA98 (Figure 2A and data not shown). Compared with wild-type +/+ mice, E12.5 *an/an* mouse sections showed a



(legend on next page)



significantly reduced number of gonocytes/primordial germ cells in the genital ridge (Figure 2A). We could not detect any aberrant located cells, i.e., cells outside the vicinity of the genital ridges. Thus, abnormal migration is unlikely the cause of germ cell depletion in *an/an* mice.

To further investigate the fate of the germ cells in *an/an* mice, we studied their proliferation and apoptosis behavior at E12.5. Here, more germ cells were positive for mitotic cell marker phospho-histone H3 (pH3) in *an/an* compared with *+/+* mice (Figure 2B). Further analysis of these mitotic cells revealed more pro/pro-metaphase cells in *an/an* compared with *+/+* mice (Figure 2B). Using activated caspase-3 as an apoptotic cell marker, we found a significant increase in apoptotic germ cells in *an/an* compared with *+/+* mice (Figure 2C). The increase in the relative number of mitotic germ cells in E12.5 *an/an* mice with more cells in pro/pro-metaphase and a lower total number of germ cells indicate a delay in mitotic progression of these cells. Intriguingly, loss of *Cdk5rap2* mutant germ cells in *an/an* mice occurs at a time when these cells physiologically exit the cell cycle and enter a mitotic quiescent phase.

Cdk5rap2 Is Required for Normal Germ Cell Cycle Progression

We then asked whether germ cell cycle progression is affected in *an/an* mice. To answer this, we performed successive pulse labeling of heterozygous (*an/+*) pregnant mice at E11.5 with two different thymidine analogs: 5-iodo-2'-deoxyuridine (IdU) and 5-bromo-2'-deoxyuridine (BrdU, interval 4 hr). Thirty minutes after the second pulse, the E11.5 embryos were collected and double immunostained with rat anti-BrdU (which detects both IdU- and BrdU-labeled cells) and mouse anti-BrdU (which specifically detects BrdU-labeled cells) (Figure 3A). This enabled us to estimate the ratio of germ cells that left the cell cycle within a time frame of 4 hr. In E11.5 *+/+* embryos, we found that many germ cells already exited the cell cycle after 4 hr, as detected by exclusive positivity for IdU (54.49% ± 3.2%). In *an/an* embryos, however, less germ cells had exited the cell cycle during the same time frame (39.02% ± 1.8%, $p < 0.01$) (Figure 3).

Our results suggest increased apoptosis as a consequence of mitotic delay and prolonged cell cycle as the likely cause

of *Cdk5rap2* mutant germ cell depletion (Figure 4). This is in line with recent studies linking mitotic delay to increased apoptosis of neuronal progeny (Pilaz et al., 2016) as well as evidence stressing apoptosis as a critical regulator of the germ cell pool (Aitken et al., 2011). In agreement with a germ cell defect in the MCPH3 mouse model, a severe reduction in testis volume due to a massive loss of germ cells has been reported in a mouse model of MCPH5 (Pulvers et al., 2010). The underlying pathomechanism may be similar to that reported here in the MCPH3 mouse model. Our findings highlight the critical role of *Cdk5rap2* in maintaining the germ cell pool during embryonic development in mice. Compared with centrosomin mutant *Drosophila* (Li et al., 1998), the stronger phenotype and the different mechanism in the mouse vertebrate model may reflect that *Cdk5rap2* has gained additional functions during evolution. We report prolonged mitosis of germ cells parallel to (and putatively leading to) massive apoptosis in the progeny as a cause of infertility. Understanding the cause leading to infertility is likewise important for understanding the fate of neural progenitors and thus mechanisms leading to microcephaly in MCPH.

EXPERIMENTAL PROCEDURES

Mice

Cdk5rap2 mutant or Hertwig's anemia mice (*an/an*) carrying an inversion of exon 4 (that leads to exon skipping [Lizarraga et al., 2010]) were generated by crossing heterozygous (*+/an*) mice (C57BL/6 background; Jackson Laboratory, stock no. 002306). The breeding was performed during the day at the animal facility of the Charité – Universitätsmedizin Berlin, Germany. The adult mice included in this study were P53-P79. Genotyping was performed using the PCR primers for (*+/+*) F 5'-TC ACT GAG CTG AAG AAG GAG AA-3', R 5'-TGT CTT TCT GCC CTG ACA GT-3' and (*an/an*) F 5'-GC AAT CAC TAA AAT GTC CGA TT-3', R 5'-TGT CTT TCT GCC CTG ACA GT-3' with an expected 1,047 bp band in *+/+*, a 500 bp band in *an/an*, and both bands in (*+/an*). All experiments were carried out in accordance with the national ethics principles (registration no. T0309.09).

Histology and Immunofluorescence Staining

After dissection, the tunica albuginea of adult testes was punctured with a needle to allow rapid penetration of the fixative (4%

Figure 2. Germ Cells in *Cdk5rap2* Mutant Mice Are Lost by E14.5

(A) MVH-positive germ cells are reduced in number in the genital ridge of E12.5 *an/an* mice and are absent by E14.5. Scale bars, 100 μm . (B) Increase in the relative number of mitotic germ cells (MVH and pH3 double-positive cells) in *an/an* mice with more cells in pro/pro metaphase. Scale bars, 100 μm (upper panel) and 10 μm (lower panel); average of 472 germ cells counted per *+/+* animal and 113 germ cells counted per *an/an* animal.

(C) Increase in the relative number of apoptotic germ cells (TRA98 and activated caspase-3 double-positive cells) in *an/an* mice. Scale bars, 100 μm ; average of 246 germ cells counted per *+/+* animal and 96 germ cells counted per *an/an* animal. Immunofluorescence images, $n = 4-5$ (E12.5), $n = 6$ (E14.5), $n = 5-6$ (P0), and $n = 6-7$ (adult) animals/group.

Error bars indicate SEM, Student's t test, * $p < 0.05$, ** $p < 0.01$, **** $p < 0.0001$.

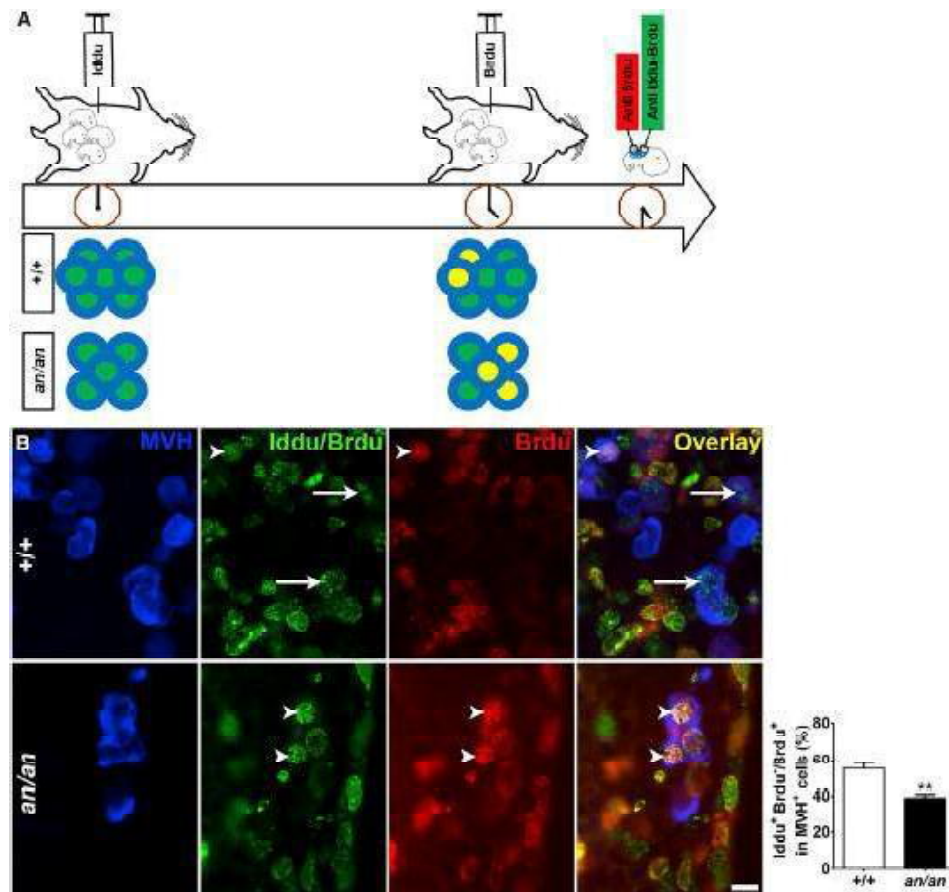


Figure 3. Cdk5rap2 Is Required for Normal Germ Cell Cycle Progression

(A) Protocol used to study cell cycle progression at E11.5 in vivo. Successive pulse labeling of heterozygous (*an/+*) pregnant mice at E11.5 with two different thymidine analogs to detect cycling cells.

(B) Decrease in the relative number of exclusively IddU-positive germ cells which left the cell cycle in *an/an* mice; green-filled circles in (A) and arrows in (B). Dual-labeled cycling cells are indicated by yellow-filled circles in (A) and arrowheads in (B). Scale bar, 10 μ m; immunofluorescence images, average of 647 germ cells counted per *+/+* animal and 182 germ cells counted per *an/an* animal, $n = 5$ animals/group. Error bars indicate SEM, Student's *t* test, ** $p < 0.01$.

paraformaldehyde in 0.12 M TPO₄ phosphate buffer). At E12.5 and E14.5, whole embryos were used. Following fixation for 10 min (P0), 4 hr (adult), or overnight (E12.5, E14.5), testes and embryos were dehydrated in an ethanol series (50%, 70%, 85%, 90%, and 100%), cleaned with xylene, and embedded in paraffin. Sections of 5 μ m were cut on a microtome and collected on Superfrost Plus slides.

P0 and adult testes sections at the position of maximal testis diameter were deparaffinized and stained with H&E. For immunostaining, deparaffinized sections were exposed to a heat-mediated antigen retrieval step with citrate-based solution (H-3300, pH 6.0), blocked in 10% donkey or goat normal serum for 1 hr at room temperature (RT) prior to incubation with the primary antibodies over-

night in a humid chamber at RT. Sections were then incubated with the corresponding secondary antibodies for 2 hr at RT, followed by PBS 1 \times rinsing and treatment with a solution containing 10 mM CuSO₄ and 50 mM NH₄Cl (pH 5) to reduce autofluorescence. Finally, the sections were washed with dd-H₂O and mounted with Immu-Mount. Primary antibodies were applied as follows: rabbit anti-MVH/DDX4 (1:500; Abcam, ab13840), rat anti-germ cell-specific antigen TRA98 (1:500; Abcam, ab82527), mouse anti-phospho-histone H3 (1:100; Cell Signaling Technology, 9706), rabbit anti-activated cleaved caspase-3 (1:200, Cell Signaling Technology, 9661), mouse anti-BrdU (1:300; Millipore, MAB3424, clone AH4H7-1), and rat anti-BrdU (1:250; Abcam, ab6326). Secondary antibodies

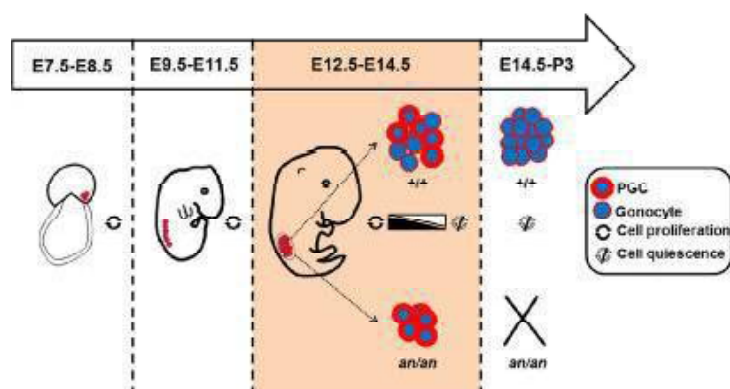


Figure 4. Schematic Model of Mechanism Leading to Embryonic Loss of Germ Cells in *Cdk5rap2* Mutant Mice

Germ cells are specified at around E7.5, proliferate, and migrate toward the genital ridge around E8.5–12.5 in mice. In *an/an* mice, germ cells undergo massive apoptosis at a time when the cells undergo physiologically mitotic arrest (E12.5–E14.5). This results in a loss of germ cells during embryonic development, which is apparent later in male infertility.

(1:400) were goat Alexa Fluor 488 conjugate anti-mouse immunoglobulin G (IgG), goat Alexa Fluor 488 conjugate anti-rabbit IgG, goat Cy3-conjugate anti-rat IgG (Invitrogen), and donkey Cy3-conjugated anti-rabbit IgG (Jackson ImmunoResearch). Nuclei were stained with DAPI (1:1000, Sigma-Aldrich).

Imaging

Bright-field images were taken with an Olympus BX60 microscope with an AxioCam MRC Zeiss camera and AxioVision 4.8 software (Zeiss). The fluorescent images were taken by an Olympus BX51 microscope with an Intas camera and MagnaFire 2.1B software (Olympus). All images were processed using Adobe Photoshop CS6 version 13.0x64.

SUPPLEMENTAL INFORMATION

Supplemental Information includes two figures and can be found with this article online at <http://dx.doi.org/10.1016/j.stemcr.2017.01.002>.

AUTHOR CONTRIBUTIONS

A.M.K. and S.Z. were responsible for the project conception and wrote the manuscript. S.Z., P.B., N.K., and G.S. performed the experiments. All authors read, revised, and approved the final manuscript.

ACKNOWLEDGMENTS

The authors thank Jessica Fassbender, Susanne Kosanke, and Magdalena John for technical assistance, Jutta Schuler for advice on microscopy, and Prof. Victor Tarabykin for discussions. This work was supported by the German Research Foundation (DFG, SFB665), the Helmholtz Association by the Berlin Institute of Health (BIH, CRG1), the German Academic Exchange Service (DAAD), and the Charité Universitätsmedizin Berlin.

Received: June 3, 2016

Revised: January 3, 2017

Accepted: January 4, 2017

Published: February 2, 2017

REFERENCES

- Aitken, R.J., Findlay, J.K., Hutt, K.J., and Kerr, J.B. (2011). Apoptosis in the germ line. *Reproduction* *141*, 139–150.
- Bond, J., Roberts, E., Springell, K., Lizarraga, S., Scott, S., Higgins, J., Hampshire, D.J., Morrison, E.E., Leal, G.F., Silva, E.O., et al. (2005). A centrosomal mechanism involving CDK5RAP2 and CENPJ controls brain size. *Nat. Genet.* *37*, 353–355.
- Buchman, J.J., Tseng, H.C., Zhou, Y., Frank, C.L., Xie, Z., and Tsai, L.H. (2010). *Cdk5rap2* interacts with pericentrin to maintain the neural progenitor pool in the developing neocortex. *Neuron* *66*, 386–402.
- De Felici, M. (2009). Primordial germ cell biology at the beginning of the XXI century. *Int. J. Dev. Biol.* *53*, 891–894.
- Fish, J.L., Kosodo, Y., Enard, W., Pääbo, S., and Huttner, W.B. (2006). *Aspm* specifically maintains symmetric proliferative divisions of neuroepithelial cells. *Proc. Natl. Acad. Sci. USA* *103*, 10438–10443.
- Issa, L., Kraemer, N., Rickert, C.H., Sifringer, M., Ninnemann, O., Stoltenberg-Didinger, G., and Kaindl, A.M. (2013). CDK5RAP2 expression during murine and human brain development correlates with pathology in primary autosomal recessive microcephaly. *Cereb. Cortex* *23*, 2245–2260.
- Kaindl, A.M., Passemard, S., Kumar, P., Kraemer, N., Issa, L., Zwirner, A., Gerard, B., Verloes, A., Mani, S., and Gressens, P. (2010). Many roads lead to primary autosomal recessive microcephaly. *Prog. Neurobiol.* *90*, 363–383.
- Kraemer, N., Issa, L., Hauck, S.C.R., Mani, S., Ninnemann, O., and Kaindl, A.M. (2011). What's the hype about CDK5RAP2? *Cell Mol. Life Sci.* *68*, 1719–1736.
- Kraemer, N., Ravindran, E., Zaqout, S., Neubert, G., Schindler, D., Ninnemann, O., Graf, R., Seiler, A.E., and Kaindl, A.M. (2015). Loss of CDK5RAP2 affects neural but not non-neural mESC differentiation into cardiomyocytes. *Cell Cycle* *14*, 2044–2057.
- Li, K., Xu, E.Y., Cecil, J.K., Turner, F.R., Megraw, T.L., and Kaufman, T.C. (1998). *Drosophila* centrosomal protein is required for male meiosis and assembly of the flagellar axoneme. *J. Cell Biol.* *141*, 455–467.



- Lizarraga, S.B., Margossian, S.P., Harris, M.H., Campagna, D.R., Han, A.P., Blevins, S., Mudbhary, R., Barker, J.E., Walsh, C.A., and Fleming, M.D. (2010). Cdk5rap2 regulates centrosome function and chromosome segregation in neuronal progenitors. *Development* *137*, 1907–1917.
- McLaren, A. (2003). Primordial germ cells in the mouse. *Dev. Biol.* *262*, 1–15.
- Megraw, T.L., Sharkey, J.T., and Nowakowski, R.S. (2011). Cdk5rap2 exposes the centrosomal root of microcephaly syndromes. *Trends Cell Biol.* *21*, 470–480.
- Moynihan, L., Jackson, A.P., Roberts, E., Karbani, G., Lewis, I., Corry, P., Turner, G., Mueller, R.F., Lench, N.J., and Woods, C.G. (2000). A third novel locus for primary autosomal recessive microcephaly maps to chromosome 9q34. *Am. J. Hum. Genet.* *66*, 724–727.
- Pilaz, L.J., McMahon, J.J., Miller, E.E., Lennox, A.L., Suzuki, A., Salmon, E., and Silver, D.L. (2016). Prolonged mitosis of neural progenitors alters cell fate in the developing brain. *Neuron* *89*, 83–99.
- Pulvers, J.N., Bryk, J., Fish, J.L., Wilsch-Bräuninger, M., Arai, Y., Schreier, D., Naumann, R., Helppi, J., Habermann, B., Vogt, J., et al. (2010). Mutations in mouse *Aspm* (abnormal spindle-like microcephaly associated) cause not only microcephaly but also major defects in the germline. *Proc. Natl. Acad. Sci. USA* *107*, 16595–16600.
- Russell, E.S., McFarland, E.C., and Peters, H. (1985). Gametic and pleiotropic defects in mouse fetuses with Hertwig's macrocytic anemia. *Dev. Biol.* *110*, 331–337.
- Western, P.S., Miles, D.C., van den Bergen, J.A., Burton, M., and Sinclair, A.H. (2008). Dynamic regulation of mitotic arrest in fetal male germ cells. *Stem Cells* *26*, 339–347.

Mein Lebenslauf wird aus datenschutzrechtlichen Gründen in der elektronischen
Version meiner Arbeit nicht veröffentlicht.

My curriculum vitae is not published for privacy reasons in the electronic version of my
thesis.

10. Complete list of publications

1. Al-hussain S, Al-saffar R, **Zaqout S**. Morphological and Quantitative Study of Neurons in the Gracile Nucleus of the Camel Brain Stem. *Journal of Behavioral and Brain Science* 2012; 1:35-47.
2. **Zaqout S**, Al-hussain S, Al-saffar R, El-dwairi Q. A Golgi Study of the Camel Cuneate Nucleus. *The Anatomical Record* 2012; 12:2191-2204.
3. Essi K, El-shafie J, Hawamdah Z, **Zaqout S**. Shoulder Pain among Rehabilitated Spinal Cord Injured Persons Using Manually Propelled Wheelchairs in the Gaza Strip: A Survey. *Disability, CBR & Inclusive Development, North America* 2012; 2:53-71.
4. **Zaqout S**, Al-hussain S. Functional and Anatomical Features of the Dorsal Column Nuclei in Mammals and Lower Animals. *American Journal of Medical and Biological Research*. 2013;1:23-27.
5. Kraemer N, Ravindran E, **Zaqout S**, Neubert G, Schindler D, Ninnemann O, Graf R, Seiler AE, Kaindl AM. Loss of CDK5RAP2 affects neural but not non-neural mESC differentiation into cardiomyocytes. *Cell Cycle* 2015; 14:2044-57.
6. **Zaqout S**, Kaindl AM. Golgi-Cox staining step by step. *Frontiers in Neuroanatomy* 2016; 10:38-45.
7. **Zaqout S**, Bessa P, Kramer N, Stoltenburg-Didinger G, Kaindl AM. CDK5RAP2 is required to maintain the germ cell pool during embryonic development. *Stem Cell Reports* 2017; 8:198-204.
8. **Zaqout S**, Morris-Rosendahl D, Kaindl AM. Autosomal Recessive Primary Microcephaly (MCPH): An Update. *Neuropediatrics* 2017; 48:135-142.

Abstracts for congress presentations

1. **Zaqout S**, Kraemer N, Fassbender J, Issa-Jahns L, Stoltenburg-Didinger G, Kaindl AM. Autosomal recessive primary microcephaly, more than just a neural progenitor proliferation defect?, Berlin Neuroscience Forum, Liebenwalde, Germany, 12-13 June, 2014 (Poster).
2. **Zaqout S**, Kraemer N, Stoltenburg-Didinger G, Fassbender J, Willerding G, Kaindl AM. Mutations in mouse *Cdk5rap2*; more than just microcephaly. 11th Göttingen Meeting of the German Neuroscience Society, Göttingen, Germany, 18-21 March, 2015 (Poster).

11. Acknowledgements

It was very important turn in my life to work on PhD project under supervision of Prof. Dr. Angela M. Kaindl, Institute of Cell Biology and Neurobiology, Charité - Universitätsmedizin Berlin. I learned from her not only how to do experiments, but also how to be efficient in working, planning and managing the time. Thank you, Prof. Kaindl, for continuously offering your support and interest for lab work as well as for my personal issues.

I thank all members of the Institute of Cell Biology and Neurobiology, Charité - Universitätsmedizin Berlin. I specially thank all of our group members for their support. Thank you, Ehtiraj Ravindran, for the nice time we expended together during the lab working days. Thank you, Bianca Hartmann, for introducing me to the cell culture and western blot techniques and for your delicious muffins which you offered for nice events. Thank you, Kathrin Blaesius, for your great help in electrophysiology experiments. Thank you, Sylvie Picker-Minh, for your feedbacks regarding my experimental findings.

I thank all of Prof. Dr. Gisela Stoltenburg-Didinger, Dr. Nadine Krämer and Dr. Olaf Ninnemann, Institute of Cell Biology and Neurobiology, Charité - Universitätsmedizin Berlin for all kind of supports. I thank Jessica Fassbender, Susanne Kosanke and Magdalena John for their technical assistance. I also thank the German Academic Exchange Service (DAAD) for their financial support for my PhD study.

All of my success during PhD years would not be possible without the hidden supports of my family. Thank you, my mother, for your continuous pray for me to reach the higher grades in education and career. Special thank to my wife for her great support at home. Thank you, my wife, for tolerating long hours of my absence, and taking care of our children which is not at all an easy job. Thank you for your delicious meals which you cooked and for trying the best to make it as healthy as possible. Thank you my kids Ismail, Ali and Sama for teaching us how to forget stress and worries by playing. Thank you for running and fighting in front of the home door to meet me first once I come back from the work.